Robustness of Bacterial Based Self-Healing Concrete Immobilized through Sisal Fiber

By

Hassan Amjad

Fall 2019-MS Structural Engineering

00000317730

Supervisor

Dr. Rao Arsalan Khushnood

NUST INSTITUTE OF CIVIL ENGINEERING (NICE), SCHOOL OF CIVIL AND ENVIRONMENTAL ENGINEERING (SCEE), NATIONAL UNIVERSITY OF SCIENCES AND TECHNOLOGY (NUST), SECTOR H-12, ISLAMABAD, PAKISTAN.

OCTOBER, 2022

This is to certify that thesis titled

Robustness of Bacterial Based Self-Healing Concrete Immobilized through Sisal Fiber

By

Hassan Amjad

Fall 2019-MS Structural Engineering

00000317730

Has been accepted towards the partial fulfillment

Of

the requirement for the award of the degree of

Master of Science in Structural Engineering

Dr. Rao Arsalan Khushnood

Supervisor

Dr. Shazim Ali Memon

Co-Supervisor

Dr. Hammad Anis Khan

GEC Member

Dr. Azam Khan

GEC Member

Thesis Acceptance Certificate

Certified that the final copy of the MS thesis written by Mr. Hassan Amjad (Registration No.00000317730) of NICE (SCEE) has been verified by the undersigned, found complete in all respects as per NUST Statutes/Regulations, is free of plagiarism, errors and mistakes and is accepted as partial fulfillment for the award of MS degree. It is further certified that necessary amendments as pointed out by GEC members of the scholar have also been incorporated in the said thesis.

Signature: ________________________

Supervisor: Dr. Rao Arsalan Khushnood

Date: ________________________

Signature (HoD): ________________________

Date: ________________________

Signature (Dean/Principal): ________________________

Date: ________________________

Declaration

I certify that this research work titled **"Robustness of Bacterial Based Self-healing Concrete Immobilized through Sisal Fiber"** is my own work. The work has not been presented elsewhere for assessment. The material that has been used from other sources it has been properly acknowledged / referred.

Signature of Student

Hassan Amjad

2019-NUST-MS-Str-00000317730

Acknowledgments

I am grateful to Almighty Allah whose countless blessings gave me the strength to accomplish this research work.

I bestow my sincere thanks to my mentor and advisor Assoc. Prof. Dr. Rao Arsalan Khushnood, department of structural engineering, NUST institute of civil engineering (NICE) for his advice, untiring guidance, incredible patience, and supervision. He inspired me through his perseverance, professionalism, diligence, and sincerity. I am grateful to him for his encouragement and motivation that urged me to achieve the best during this research program.

I would like to thank my co-supervisor and research committee members: Dr. Shazim Ali Memon, Dr. Hammad Anis Khan and Dr. Azam Khan for their support during my research.

I extend my gratitude and special thanks to my seniors specially Miss Nafeesa Shaheen, and Miss Maria Kanwal, PhD Candidates (NICE), who extended their unconditional guidance, precious time and valued input towards my research

I also acknowledge the support provided by lab staff at NICE Structural engineering lab for my extensive experimental work.

Lastly, I am thankful to my parents and friends especially Muzzamil and Zaheer, for bringing vital dose of moral support and encouragement, week in and week out.

Dedicated to my exceptional parents, especially to my beloved mother for the endless love and prayers that led me to this wonderful accomplish.

Abstract

Bio-healing is now believed as a promising technique for the repair of concrete cracks. However, the healing capability of bacterial mixes against repeated damage cycles is still questionable. This study aims to investigate the robustness of bio-healable concrete against two successive damage cycles using *Bacillus Subtilis* immobilized via sisal fiber. The formulated bio-concrete exhibited improved mechanical properties and attained a maximum of 13.96% and 36.82% enhancement in terms of compression strength and split tensile strength. Self-healing efficacy was assessed by quantifying the average crack healing width and the recovered strength in compression during the healing phase. Results revealed that sisal fiber efficiently preserves spores of the bacillus strain and enhances its bio-metabolic potential to precipitate calcite for sealing concrete cracks. The average crack of 0.48 mm width was successfully healed in the first damage cycle whereas the complete repair of a 0.28 mm wide crack on average was attained in the healing phase of the second damage cycle. The maximum recovered compressive strength was 82.65% and 50.42% in the two successive damage cycles through bio-healing. The crack-healing precipitate was identified as calcite crystals through forensic examination. Consequently, immobilizing *Bacillus Subtilis* with sisal fiber was proved as a viable approach for improving the mechanical properties of concrete and inducing robust self-healing in repeated damages.

Key Words: Self-healing concrete, Bacillus Subtilis, Sisal fiber, Autonomous healing, Rigor healing, Multiple damages

LIST OF ABBREVIATIONS

OPC	Ordinary Portland Cement
ASTM	American Society for Testing and Materials
SF	Sisal Fiber
TSB	Tryptone Soya Broth
BS	Bacillus Subtilis
OD	Optical Density
BISF	Bacillus Subtilis Immobilized in Sisal Fiber
TGA	Thermal Gravimetric Analysis
FTIR	Fourier Transformed Infrared
SEM	Scanning Electron Microscope
EDS	Energy Dispersive Spectroscopy
XRD	X-ray Diffraction
RCS	Recovered Compressive Strength
UPV	Ultrasonic Pulse Velocity
HE	Healing Extent
PCM	Plain Control Mix
FCM	Fiber Control Mix
PBM	Plain Bacterial Mix
FBM	Fiber Bacterial Mix

TABLE OF CONTENTS

LIST OF FIGURES

LIST OF TABLES

1 INTRODUCTION

1.1 Theoretical Background

Concrete is the most commonly used construction material because of its remarkable qualities, such as ease of casting, great compressive strength, and cost-effective performance. However, due to its brittleness and low tensile strength, this material is prone to cracking in a variety of situations, including the presence of high stresses from an external load, thermal expansion, creep, shrinkage, expensive reactions (such as the alkali-aggregate reaction (AAR), embedded steel corrosion, etc.), and aggressive environmental exposure [1,2]. The greatest detrimental factor that affects concrete's durability is thought to be cracking. These cracks also account for the reduction in concrete strength due intrusion of harmful chemicals such as SO_4^{-2} and Cl^{-1} from the surrounding environment. This will elicit corrosion and drop the structure's durability, potentially causing safety hazards and reducing the overall structural life of the building [3,4]. Numerous repair techniques broadly classified as manual and self-healing repair; are utilized to heal cracks in concrete and diminish or even eradicate the degradation of concrete. The external interventions are labor dependent and cost intensive. Furthermore, they have compatibility problems since a weaker connection was observed at the repair site, and their processing is harmful to the environment [5,6]. As a result, researchers are exploring long-term crack mitigation options to decrease costs and environmental consequences. The latest research carried out over the last decade focus on how to enhance the durability and performance of concrete. This resulted in the invention of self-healing concrete (SHC) that has an intrinsic property to repair the cracks by itself. The intrinsic self-healing technique in concrete manifested into autogenous and autonomous healing. Autogenous healing occurs due to the secondary hydration of anhydrous cement particles and the formation of calcium carbonate ($CaCO_3$) crystals due to some chemical processes [2]. Healing due to the addition of external agents like micro-organisms, micro-vascular and tubular capsules, and engineered composites in the concrete matrix are categorized into autonomous healing [7,8]. Concrete can be made less susceptible to cracking by the addition of some micro/macro fibers [9–11]. With the contribution of fiber and biotechnology in cementitious materials, healing can be further fortified with improved engineering properties. Recently, the sustainable technique of self-healing via microbial precipitated $CaCO_3$ termed bacterial-based self-healing has been comprehensively studied to heal cracks [7,12]. Moreover, self-healing material must satisfy several robustness requirements like long shelf life, pervasiveness, stability, reliability, versatility, and repeatability [13]. In this work, robustness refers to the repeatability of healing.

1.2 Self-Healing Concrete

It is a term used to describe the automatic repair of nano-micro cracks in concrete that develop over the service life of buildings. Various measures are attempted to prevent and heal these cracks. Due to the improved engineering properties of fiber-reinforced concrete, its crack inhibition effect, and recent advancements in microbiology, biological healing agents with fibers in cementitious materials have taken an interest to promote self-healing. Fibers are helpful in the inhibition of crack propagation, thus substantially adding to the robust crack healing of concrete.

1.2.1 Bacterial-based concrete

Concrete that uses certain microorganisms for healing is known as bacterial-based self-healing concrete. During their ureolytic or non-ureolytic activities, bacteria discrete the $CaCO_3$ precipitates [10]. Recent studies have shown a lot of interest in bio-based self-healing techniques. It is recommended that bacteria should always be incorporated into the concrete through carrier media for their prolong survival [16].

1.3 Fibers in concrete

Different fibers can be used in concrete like carbon, basalt, polypropylene, polyvinyl alcohol, glass & natural fibers. It has been found that all these fibers improve the mechanical properties of concrete, restrain cracking, improve fire performance & reducing shrinkage [17–23]. According to numerous studies, using natural fibers to strengthen concrete is a practical and affordable alternative to traditional building materials [17,18,24–27]. It has been determined that natural fibers are potential components of composites used in building materials and other applications [10]. Particularly, natural fibers have the following favorable characteristics [26,28]:

- Natural fibers are widely known and available all over the world and can easily be cultivated.
- They have a low carbon footprint as they are typically extracted as either primary or secondary byproduct material and do not require as much processing as when artificial fibers are manufactured. Thus, they have little negative effects on the environment.

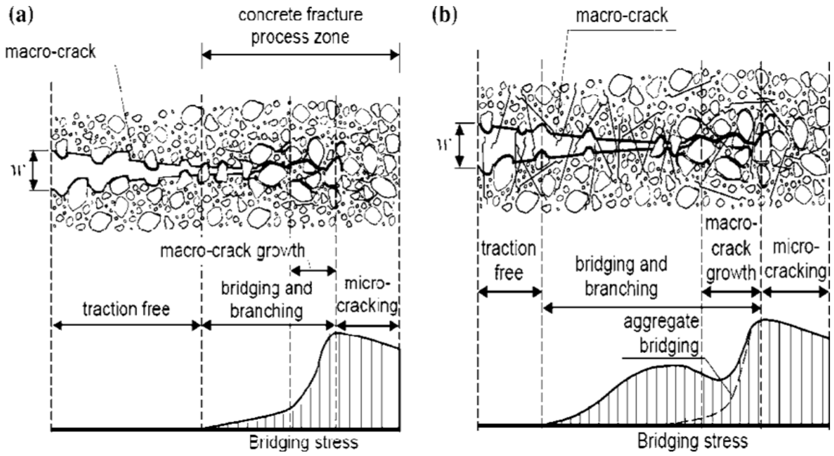

Figure 1-1 Fiber reinforcement effect in concrete (Löfgren, 2005)

1.4 Materials for Bacterial-based Self-Healing Concrete

1.4.1 Bacteria

Bacteria are small-cell microorganisms that may be found everywhere, including the human body, air, and food. There are several bacterial species, some of which are extremely hazardous to humans while others are quite beneficial. They are classed according to their shape, size, morphology, and appearance. Numerous bacterial species are employed for a variety of applications, including food, medicine, and cementitious systems. Bacteria with the ability to precipitate $CaCO_3$ are extremely beneficial in producing robust concrete.

1.1.1.1 Bacillus Subtilis (BS)

BS bacteria is a rod-shaped, non-ureolytic bacteria found in the soil and gastrointestinal tract of human bacterial. This specie of bacteria can persist in highly alkaline environments and therefore is mostly employed in bio-concrete. The bacteria when incorporated directly into concrete can remain viable for up to 4 months.

By adding certain salts, the BS may be transformed into spores and can endure in the dormant state for a longer period.

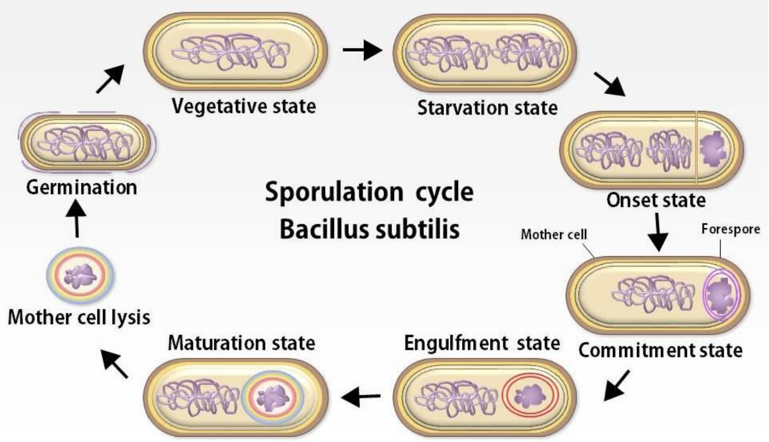

Figure 1-2 Sporulation process in BS

They interact with moisture coming from empty spaces or nano-micro fractures in the presence of certain nutrients, precipitating calcite in concrete pores and cracks. The calcite accelerates the crack-healing process. Compared to many other ureolytic bacteria, it has a greater capacity to speed up the biosynthesized $CaCO_3$ precipitation [3]. As a result, this phenomenon leads to concrete structures that are less porous and more robust.

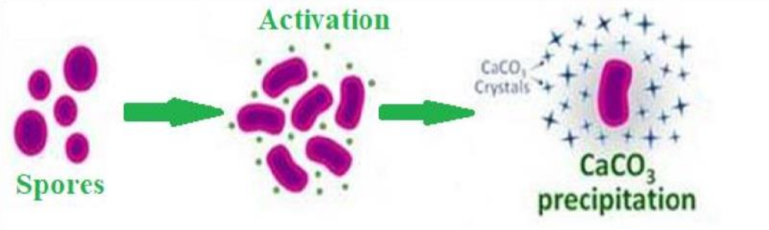

Figure 1-3 Calcite precipitation by bacterial spores

1.4.2 Sisal Fiber (SF)

It is composed of cellulose, hemicellulose, and lignin is obtained from the leaves of the sisal plant (Agave Sisalana). About 4% of fibers are yielded from the leaves of the sisal plant [29]. Because these fibers are harvested and shredded from plant leaves, they have an extremely low carbon footprint when comparison to other fibers [28,29], therefore it must be utilized in order reduce the global carbon emissions. It is cultivated in the countries like Brazil, Kenya, Tanzania, South Africa, China, and Mexico. According to Broeren et al. [30], Brazil is the world's leading producer and exporter of

SF, accounting for 58% of the production and 70% of the global exports. As reported by FAO 2022 [31], global SF production was 233.7 kt/y.

Figure 1-4 Agave Sisalana plant

SF possesses great mechanical properties, low environmental impact, and has the least cost which has previously been investigated for improving cementitious materials performance [32–35].

Properties	**Sisal**
Density(g/cm^3)	1.33-1.45
Tensile strength	510-700
Young's modulus(GPa)	9-38
Moisture absorption %	11
Elongation at break (%)	2.2-2.9

Figure 1-5 Mechanical properties of SF (Ren et al. 2022)

Because of its hydrophilic nature, it can act as a potential immobilizer for bacteria in bio-concrete [2,15,36]. The immobilization technique which protects bacterial spores from crushing during mixing and hydration reactions leads to the better pervasiveness of microbes and the fiber reinforcement effect which mitigates crack propagation can significantly enhances the robustness of self-healing concrete.

1.5 Objectives

Keeping in view the above-mentioned problems, this research has the following objectives:

- Investigate the potential of SF as a suitable immobilizer for BS in bio-based self-healing concrete
- Investigate the healing efficacy of the formulated concrete in two successive crack cycles.

1.6 Significance of this Research

Structures are always subjected to multiple loading some of which repeatedly act on the structures resulting in the widening of the existing cracks in the structures. These cracks if not healed will continue to widen and thus ultimately will decrease the life span of the structure. The bacterial-based self-healing concrete can significantly improves concrete durability. Moreover, this also allows the concrete to heal the cracks without human any intervention because of bacterial inherent catalytic metabolism that precipitates carbonate minerals. Adding fibers into the concrete not only improves greatly improves concrete properties but also prevents crack propagation. Immobilizing bacteria through BS which is a natural fiber, therefore, provides a sustainable and environmentally friendly technique to self-repair cracks and thus enhance the durability of the structure. Besides, these additives in concrete can lead to making a more durable, self-healing, and economical composite having negligible serviceability problems. Several robustness characteristics, including long shelf life, pervasiveness, stability, reliability, versatility, and repeatability, must be met by a self-healing material. The immobilization method that improves microbial survival and the fiber-reinforcing effect that inhibits crack propagation can therefore increase the resilience of self-healing concrete.

2 LITERATURE REVIEW

2.1 Self-Healing Concrete

It was observed in 1836 that conventional concrete with w/c ratios ranging from 0.4 to 0.55 may heal small cracks by itself. About 70% of the cement reacts during the hydration phase, with the remaining 30% unreacted in the paste [37]. The remaining unreacted cement then interacts with the moisture in the cracks, filling them with hydration products. As a result of un-hydrated cement particles interacting in the presence of moisture after cracking, clogging of cracks by detached loose particles, or $CaCO_3$ formation due to interaction of $Ca(OH)_2$ with dissolved CO_2 in water autogenous healing may occur [4,6]. Most investigations affirm that the healing product in case of autogenous healing was calcite, C-S-H, and portlandite, which begin developing from the walls of the cracks towards the middle of the crack thereby closing the crack mouth [3,38]. The governing equation for the reaction is:

$$Ca(OH)_2 \rightarrow CaO + H_2O \tag{2.1}$$

$$CaCO_3 \rightarrow CaO + CO_2 \tag{2.2}$$

This process is slow, and only small width cracks below 0.3 mm can be healed [38,39]. Subsequently, additional substances like engineered cementitious minerals, crystalline admixtures, polymers, super absorbent polymer (SAP), shape memory alloys, and microbes were added to the cementitious to improve the self-healing process by effectively filling wider cracks [1,13,40,41].

Mineral admixtures have been utilized in concrete for flexural resistance, pore refinement, strength, durability, shrinkage compensation, and enhancement in the interfacial transition zone [42]. Since nanoparticles have a larger area-to-surface ratio, they are indeed a promising candidate to add an inherent self-healing property to cementitious composites [43,44]. The crack-healing efficacy of conventional portland cement mortar (OPC) and blast furnace slag mortar in artificial seawater and freshwater was compared [45]. In freshwater, blast furnace slag outperformed OPC mortar by 100% of healing cracks up to 0.408 mm and 0.168 mm, respectively, however in seawater, OPC outperformed blast furnace slag by healing 0.104 mm and 0.592 mm cracks, respectively. However, mineral healing terminates when the healing agent is consumed, primarily in hydration processes, therefore the fundamental requirement of repeating healing cannot be achieved [44].

For the self-healing of cracks, various vascular and micro-encapsulated self-healing materials such as polymethylmethacrylate, starch, inorganic phosphate cement, and alumina were also investigated [5,46–48]. Using these techniques for inducing self-healing in concrete, the utmost 0.300-0.500 mm closing of cracks can be observed [49]. However, the disadvantage of this healing process is its significantly lower strength due to a weak interfacial zone between the capsules and the concrete matrix [50]. Furthermore, healing was just evident in the vicinity of capsules [13,51]. SAP commences the self-healing mechanism through reduced cracking caused by self-desiccation and autogenous shrinkage, as well as its self-expansive tendency, which results in pore plugging. However, the main disadvantage of SAP is its reduced compressive strength [47,48]. Shape memory alloys (SMA) are used in concrete technology to improve mechanical performance while also inducing smart sensing, dissipating, healing, and thermostatic capabilities [52]. Furthermore, the ability of SMA to control the shape and initiate the transition under heat, pH, light, and electric fields is a potential use of SMA at the nanoscale that can enhance structural performance [53]. However, the high expense and specialist labour makes it unsuitable for use in concrete buildings.

Microorganisms, such as fungi and bacteria are employed to mediate cracks within cementitious systems [54,55]. This healing mechanism is activated by the presence of moisture and air near the crack [7,12]. Bacteria can remain dormant for up to 200 years before becoming active upon exposure to moisture and air [15]. Self-healing via microorganisms is commonly employed due to accruing benefits such as $CaCO_3$ precipitation, which promotes strength and utilizes vast volumes of CO_2, which is responsible for air pollution and steel corrosion [4,56,57].

2.1.1 Bacterial-based Self-Healing Concrete

In 1998, Ramakrishnan and coworkers [58] first proposed the notion of concrete crack repair with the inclusion of microorganisms. Bacillus Pasteurii and Sporosarcina bacteria were used by the researchers to heal mortar samples that had been artificially cracked. Later, in 2005, Ghosh, Mandal, Chattopadhyay, and Pal [59] utilised E. coli bacteria to enhance the strength of cement mortar. In 2007, Jonker [60] directly intruded bacteria into the concrete mix to develop a homogeneous autonomous healing mechanism. Similarly, a two-component self-healing concrete was developed employing Bacillus Pseudofirmus and Spoosarcina Pasteurii bacteria cultivated from high alkaline water bodies to accelerate the conversion of organic compounds to calcite [61,62]. The healing efficacy of a bacterial-based healing system depends on the biosynthesis of $CaCO_3$, which is connected to bacterial type, precipitation mechanism, nutrient availability, and pH of the system [1,63]. The availability and concentration of oxygen, curing techniques, and the material employed to immobilize bacteria are other factors [7,64]. Compressive strength decrease and a slowing self-healing rate over time are the two primary problems with bacterial-based self-healing concrete. These are mainly linked to bacterial mortality and crushing during the concrete mixing and hardening stages [3,5,16].

Calcite deposition in the environment is caused by both autotrophic and heterotrophic calcifying microorganisms. However, because autotrophic bacteria struggle to survive and have a reduced rate of precipitated calcite, they have not yet been studied in cementitious systems [65]. In reality, self-healing efficacy is determined by bacterial survival and the capability for calcite deposition. Because of their ability to survive at alkaline pH, heterotrophic soil bacteria such as Bacillus, Pseudomonas, Sporosarcina, Shewanella, and Escherichia are commonly used in cementitious systems [1,66,67]. Bacillus species are prominent in showing self-healing efficacy due to their capability to produce spores [68,69]. Bacillus strains with ureolytic and non-ureolytic activity precipitate $CaCO_3$. Ureolytic bacteria release urease enzymes, which are utilized to hydrolyze urea, and the bacteria precipitate CO_2 and ammonia. If enough calcium is available, CO_2 in the presence of water forms $CaCO_3$ [10]. The underlying process of ureolytic activity of bacteria resulting $CaCO_3$ is shown below:

$$CO(\mathrm{NH_2})_2 + H_2O \rightarrow \mathrm{NH_2COOH} + \mathrm{NH_3} \tag{2.3}$$

$$\mathrm{NH_2COOH} + H_2O \rightarrow \mathrm{NH_3} + +H_2CO_3 \tag{2.4}$$

$$HCO_3{}^{-1} + H^+ + 2NH_4{}^+ + 2OH^- \rightarrow CO_3{}^{-2} + 2NH_4{}^+ + H_2O \tag{2.5}$$

$$Ca^{+2} + HCO_3{}^{-1} + OH^- \rightarrow CaCO_3 + H_2O \tag{2.6}$$

Whereas below reactions show non-ureolytic bacteria producing $CaCO_3$ due to their metabolic activity in the presence of calcium source as bacterial food and oxygen [15]:

$$CaC_6H_{10}O_6 + 6O_2 \rightarrow CaCO_3 + 5H_2O + 5CO_2 \quad (2.7)$$

Additionally, the resulting CO_2 reacts with the portlandite ($Ca(OH)_2$) and speeds up the autogenous healing process. Greater concentrations of calcite may be produced by bacterial based self-healing concrete, which enables greater crack widths to be healed by itself [12,16].

A self-healing concrete consisting bacteria can improve the mechanical properties of both undamaged and damaged concrete. Ghosh et al. [59] employed Shewanella Specie and compared it to E. coli in cement mortar at concentrations of 10^3, 10^5, and 10^7 cells/ml. Compressive strength was increased by 25% when 10^5 cells/ml were used, while no strength gain was seen in the case of E. Coli. Muynck et al. [70] used Bacillus sphaericus strains and found that urea hydrolysis increased durability. Jonker investigated the survivability of Bacillus pseudofirmus and Bacillus cohnii in cement mortars over 4 months through active pathway [71]. George discovered that urea hydrolysis was effective for calcite precipitation when S. pasteurii was utilized at varied cell concentrations ranging from 10^6 to 10^8 cells per ml [72]. In terms of compressive strength, Sujatha et al. employed soil isolate and found that urea and plain water curing improved by 18 to 12% [73]. For use in the cementitious matrix, Ghosh et al. [74] examined the spore-forming capacities of Bacillus megaterium and BS. To enhance the mechanical performance of cement, Xu et al. [75] tested non-ureaolytic bacterial strains using flexural, ultrasonic pulse velocity, and nano-indentation methods. A transition zone served as a strong link between the matrix and the calcium glutamate layer that was formed, with its average nanomechanical values being around 20% higher than those of the outside precipitates. BS was utilized in concentrations of 5 ml, 10 ml, 15 ml, and 20 ml by Arulsivanantham et al [76]. They found that greater bacterial concentrations result in more calcite production, resulting in a higher compressive strength was seen in the 20 ml replacement. Further extending his research, Kumar et al. [75] took replacement up to 30 ml and validated the same pattern [90]. To achieve 0.8mm healing and water tightness, Luo et al. [77] employed cement paste systems containing 10^9 cells/ml spore-forming bacteria. Later, he used three distinct calcium sources to conduct further investigation on the rheological characteristics [78]. Bacillus pseudofirmus was employed by Lors et al. to enhance the healing response [79]. Bacillus megaterium was utilised by Andalib et al. [92]; they found that the ideal concentration was 30 x 10^5 cfu/ml and that compressive strength increased by 24%. Based on compressive strength, Bashir et al. [79] examined the effectiveness of Bacillus pasteurii, B. Subtilis, and B. sphaericus utilising urea and carbonic salts. They found B. sphaericus to have the highest compressive strength. Bacillus sphaericus was employed by Sahoo et al. [80] at a concentration of 10^7 cells/ml, and they saw a 28% improvement in strength at this concentration combined with an accelerated rate of strength growth in SHC. E. coli and Sporosarcina pasteurii were employed in a different study at varying doses. While S. pasteurii enhanced maximal strength at 10^8 cells/ml, E. coli had little effect on strength [67]. Bacillus sp. was utilised by Joshi et al. [81] via urea hydrolysis, and substantial resistance to sulphate attack was note .

Numerous bacteria have been employed in concrete to improve microstructure and crack healing, increasing durability. BS are among the finest bacteria because they have excellent spore-forming abilities, are compatible with concrete due to their alkaliphilic nature, can persist in a dormant state for a very long time, and effectively improve mechanical performance [3,69,82,83].

2.1.2 Bacterial Immobilization in Bacterial-based Self-Healing Concrete

The bacteria can be incorporated into concrete either directly which remains viable for up to 4 months or through immobilization technique i.e. encapsulation and absorption. According to numerous research, bacteria when directly intruded in concrete had a significantly lower concentration of spores than those immobilized by a carrier [5,6,12,16,36,71,84] This implies that the immobilization of bacterial spores is beneficial in keeping them for a longer period in cementitious composites. Immobilization helps to protect bacteria in severe environments such as alkaline pH and to protect during concrete mixing and curing.

Numerous research has been done to investigate potential alternatives for successfully immobilizing bacteria in cementitious systems for longer periods. Bacteria spores embedded in silica gels and inorganic oxides before being mixed in concrete have been demonstrated as a suitable technique for extending bacterial life without affecting compressive strength [85]. In another study, the ceramsite carrier was utilized to immobilize bacteria and nutrients individually, resulting in a successful increase in crack area healing rate of up to 87.5%, as well as an increase in mechanical characteristics [86]. Khaliq and Ehsan [16] found that when LWA and graphite nano-platelets were used as carrier media for BS improvement in the compressive strength and maximum healing of 0.61 mm and 0.81 mm was observed. In another investigation, expanded perlite (EP) immobilization was compared to direct induction and bio-immobilized expanded clay (EC) [43]. Experiments revealed that EP-immobilized bacteria showed effective crack healing up to 0.79 mm compared to EC-immobilized self-healing concrete with a maximum crack healing width of 0.45 mm [12]. Immobilized bacteria via zeolite were employed in RCC and fiber-reinforced mortar to examine microstructural and crack healing capabilities [66]. This approach demonstrated an improvement in compressive strength with a decrease in chloride ion penetration. A study conducted on limestone powder proves it as a potential immobilizer for BS [87]. By incorporating Sporosarcina pasteurii ATCC 11859 into the mix using low alkali cement, Xu et al. 2018 [88] observed that compressive strength and water tightness had increased by 130% and 50%, respectively, as compared to ordinary mortar. Shaheen and Khushnood [1] found that intrusion of iron oxide as an immobilizer for BS can completely heal cracks up to 1.2 mm with 85% strength recovery. Utilizing rubber particles as a carrier media can heal cracks to about 0.86 mm width as reported by Xu and Lian [89]. Recycle brick and biochar also prove to be suitable carrier media for BS [3,15]. A maximum of 0.92 mm healing with a strength recovery of 69% was observed in the case of recycled brick while biochar showed healing of 0.50 mm and 95% strength recovery. Vijay & Murmu [90] amalgamated basalt fiber at the dosage of 4.05 kg/m^3 in bacterial concrete and affirmed higher strength recovery after healing of about 83.3%, compared to 69.25% in the control sample. Feng et al. [91] incorporated PP and PVA fiber at 1.5% by volume in bacterial concrete and concluded that the synergetic effect of synthetic fiber and bacteria can recover the initial sorptivity by more than 50% and flexural strength ranging from 16-34% compared to reference undamaged samples. In addition, bacterial fiber reinforced concrete showed 64.6% sealing for 0.3-0.5 mm crack width, compared to 30% in the control sample at 28-day healing. A similar study was also conducted by Su et al. [92] who incorporated PP fibers by 1.5% in volume carrying Bacillus alcalophilus spores and achieved 96% sealing for 0.4-0.5 mm crack width, compared to 40% in the control sample due to autogenous healing at the age of 28-day. It was found that after 28 days healing, capillary water absorption was significantly lowered in the mortar with bacteria and fiber followed by mortar with bacteria and the control samples. Furthermore, bacteria contributed to add in the flexural strength retention of PP-reinforced mortar by 4%. Singh & Gupta [36] incorporated UltraFiber 500 cellulose fibers at 0.5% by volume carrying BS in cement mortar and investigated its self-healing efficacy through ultrasonic pulse velocity. Their study affirmed that after 21 days healing, 15.2% of self-healing was attained in specimens with cellulose fiber as a carrier to BS, compared to 6.97% in the control sample. Rauf et al [10] analyzed the efficacy of natural coir, flax, and jute fibers as the potential immbolizer to BS, Bacillus cohnii, and Bacillus Sphaericus. The study reported that the investigated natural fibers offer better preservation sites to immobilized bacteria due to their high sorption capacity and internal structure. Flax fiber was the optimized immobilizer for preserving long-term bacterial activity in concrete owing to 0.8 mm of maximum crack healing with 60-100% of compressive strength recovery in damaged samples.

2.2 Concrete reinforcement with fibers

Concrete can be made less susceptible to cracking by the addition of some micro/macro fibers [10,21,22] They help inhibit crack propagation, thus making crack healing in concrete easier to attain [93]. Different fibers can be used in concrete like carbon, basalt, PP, PVA, Glass & natural fibers [18,20–22,27,28,94,95]. Nowadays, the potential of natural fibers is being studied for their use in cementitious materials [10,28]. To promote the use of natural fibers in structures, Femandez [96] optimized flax fiber reinforced concrete. The research aimed at the optimal length and ratio of flax fibers in concrete to achieve its most benefits. The fiber length was optimized at 3 cm. Tensile and compression strength testing on cylindrical specimens was carried out, and small beams were employed for three-point bending tests. The results revealed that the strength and toughness of flax fiber-reinforced concrete improved significantly. Yalley and Kwan [97] conducted an investigation on coir fiber for improving concrete properties. Coir fibers with diameters ranging from 0.29 mm to 0.83 mm and lengths ranging from 6 mm to 24 mm were employed in the experiment, resulting increase in the angle of twist. Concrete with 0.5% fiber content had the highest compressive strength, tensile strength, and torsion. Razmi and Mirsayar [98] examined the fracture characteristics of concrete reinforced with jute fiber. Jute fiber was incorporated into the concrete in increments of 0.1%, 0.3%, and 0.5% by weight while keeping a 20 mm length. Concrete specimens with semicircular bends were made. The results showed that adding 0.5% jute fiber to the mix significantly improved its compressive, flexural, and split tensile strengths. Fracture resilience was also improved, although not significantly in combinations containing more than 0.3% jute fibers.

SF, a naturally derived fiber obtained from the leaves of the agave sisalana plant, is an eco-friendly and cost-effective material that can be utilized in an effective way to reduce global carbon emissions. According to FAO 2022 [31], global SF production in 2022 was 233.7 kt/y. It possesses great mechanical properties, low environmental impact, and has the least cost which has previously been investigated for improving cementitious materials performance [32–35,99,100]. Abirami et al. [33] investigated the mechanical properties of M40-grade concrete with sisal and Kenaf fiber. Fibers were incorporated into the concrete in increments of 0.25%, 0.50%, 0.75%, and 1.00% by weight while keeping a 60-80 mm length. The results showed that adding 1.0% sisal fiber to the mix significantly improved its compressive, and split tensile strengths by 4.04% and 12.70%. Mbereyaho et al. [101] conducted a similar investigation on M30-grade concrete with 0.50%, 1.00%, and 1.50% by volume SFof 50 mm length. The compressive and tensile strengths of M30 concrete with 1% SFs were found to be 14.32% and 12.26% higher, respectively. Ren et al. investigated SF on the mechanical properties of ultra-high performance concrete at different lengths (6, 12, and 18 mm) and volume contents (1.0%, 2.0%, and 3.0%). He came to the conclusion that 1.0% SF of 18 mm when added to the mix substantially enhanced its compressive strength. However, beyond that, its compressive strength declines, but its flexural strength and toughness still increase. Solai Mathi et al. [102] also reported that the use of SF improved the mechanical performance of concrete. Tunje et al. [103] investigated the effect of SF at 0.50%, 1.00%, 1.50%, and 2.00% by weight increments on sugarcane bagasse ash concrete. He discovered that SF at 1.00% increased compressive strength by 17.22% and tensile strength by 39.58%. An experimental investigation by Shah et al. [24] was conducted to determine the fiber reinforcement effect incase of high-strength concrete. The findings showed an increase in compressive and tensile strength with 1% SF by weight and a length of 20 mm. Improvement in the impact resistance and compressive strength of SF hybrid reinforced concrete by Naraganti et al. [18] was also revealed. Another study, done by Ren et al. [19] demonstrates that SF have a positive impact on the mechanical properties of ultrahigh-performance concrete, with a substantial improvement shown when employed in hybridization with steel fibers. The study also found an improvement in post-fire residual mechanical properties due to the reinforcing effect provided by fibers.

Above mentioned, research supports SF's compatibility with concrete matrix, which helps to strengthen it effectively. Therefore, it is worthful to investigate its potential as a successful carrier of microbial strains in concrete. Because of its hydrophilic nature, it can act as a potential immobilizer for bacteria in bio-concrete [2,15,36]. The immobilization technique which protects bacterial spores from crushing during mixing and hydration reactions leads to the better pervasiveness of microbes and the fiber reinforcement effect which mitigates crack propagation can significantly enhances the robustness of self-healing concrete.

2.3 Robust self-healing concrete

A self-healing material must satisfy several robustness requirements like long shelf life, pervasiveness, stability, reliability, versatility, and repeatability [13]. In this work, robustness refers to repeatability after the first healing cycle. Thao and Johnson [104] studied isocyanate pre-polymer (epoxy) as a healing agent encapsulated in the reinforced concrete beam in terms of recovery of strength and stiffness for the first and second healing cycle. Their findings showed 88% and 85% of normalized stiffness recovery for the first and second healing cycles, compared to reference pre-damaged samples when the initial crack widths were kept at around 0.30 mm. The self-healing potential of polyurethane foam and superabsorbent polymers after two damage cycles had also been investigated [13,105]. It was affirmed that about 61% and 23% of flexural strength recovery was found for polyurethane foam healing agents, compared to reference pre-damaged samples. Superabsorbent polymers, when used as a healing agent, showed 75% and 66% of flexural strength recovery, compared to reference pre-damaged samples. A detailed investigation on self-healing triggered by crystalline admixtures under repeated cracking and healing cycles for three healing exposure conditions and one-year duration was done by Cuenca and Tejedor [106]. Their findings showed complete sealing of cracks having a width of 0.30 mm down. A similar study using biochar-immobilized bacteria and superabsorbent polymers was performed by Kua et al. [6] reporting a 4% and 19% decrease in bacterial activity for crack healing during the secondary and tertiary damage cycles. The literature evidence that fibrous cement matrix provides a more conducive condition to immobilize bacteria through fibers [10]. Therefore, the investigations need an extension to explore the potential of bacteria carried through fiber in repeated damage cycles.

2.4 Research Gap

Considering the abundance and mentioned properties of natural SF it is worthful to investigate its potential as the successful carrier of microbial strains in concrete. Since the literature evidence that fibrous cement matrix provides a more conducive condition to immobilize bacteria through fibers. Therefore, the investigations need an extension to explore the potential of bacteria carried through fiber in repeated damage cycles. The scope of the present work is to investigate the potential of SF as a suitable immobilizer for BS in bio-based self-healing concrete and the analysis of its healing performance in two successive damage cycles.

3 MATERIALS AND METHODOLOGY

3.1 Materials

3.1.1 Concrete

In this study, ordinary portland cement (OPC) meeting the guidelines as per ASTM C-150 [107] was utilized as a key binding agent of concrete. Its physical properties and chemical composition are summarized in Table 3-1; where the chemical constituents were measured by the X-ray fluorescence (XRF) technique. The physical properties of fine and coarse aggregates in compliance with ASTM C33 [108], ASTM C127 [109], and ASTM C128 [110] are given in Table 3-2.

Table 3-1: Physical properties and chemical composition of OPC

Chemical composition (oxides)	Content (%)	Physical properties	Results
CaO	63.58	Specific gravity	3.14
SiO_2	21.9	Specific surface area	321 (m^2/kg)
MgO	2.56	Consistency	29.15%
Al_2O_3	5.10	Initial setting time	185 min
Fe_2O_3	4.10	Final setting time	241 min
SO_3	2.74	Soundness	0.103%
Na_2O	0.23	Grade	42.5
K_2O	0.88	Finess modulus	93.30%
Loss on ignition	0.63	-	

Table 3-2: Physical properties of fine and coarse aggregates

Aggregates	Bulk Specific Gravity	Fineness Modulus	Absorption (%)
Fine	2.75	2.90	2.15
Coarse	2.68	-	0.72

3.1.2 Preparation of BS spores' solution

Colonies of BS were first cultured on agar media plates after that inoculation in Tryptone Soya Broth (TSB) is done. The TSB was incubated for 24 h at 37 ˚C in a shaker, resulting in dramatic growth in BS cells. A sporulation medium consisting of

$Ca(NO_3)_2$ (1.0 mM), $FeSO_4$ (0.001 mM), KCl (13.4 mM), $MnCl_2$ (0.01 mM), and $MgSO_4.7H_2O$ (1.01 mM) was added in bacterial TSB solution and again shaking incubation for 5 days at 37 ˚C was continued at 120 rpm [10]. Cells were pelleted by centrifuging at 4000 rpm speed and 6˚C temperature for 20 min. Extracted spores were suspended in sterilized distilled water and optical density (OD) was adjusted to 0.5 to get the desired BS spores' solution (SS). The 0.5 OD was chosen in accordance with the previous studies [3,10]. The detailed schematic procedure is described in Figure 3-1.

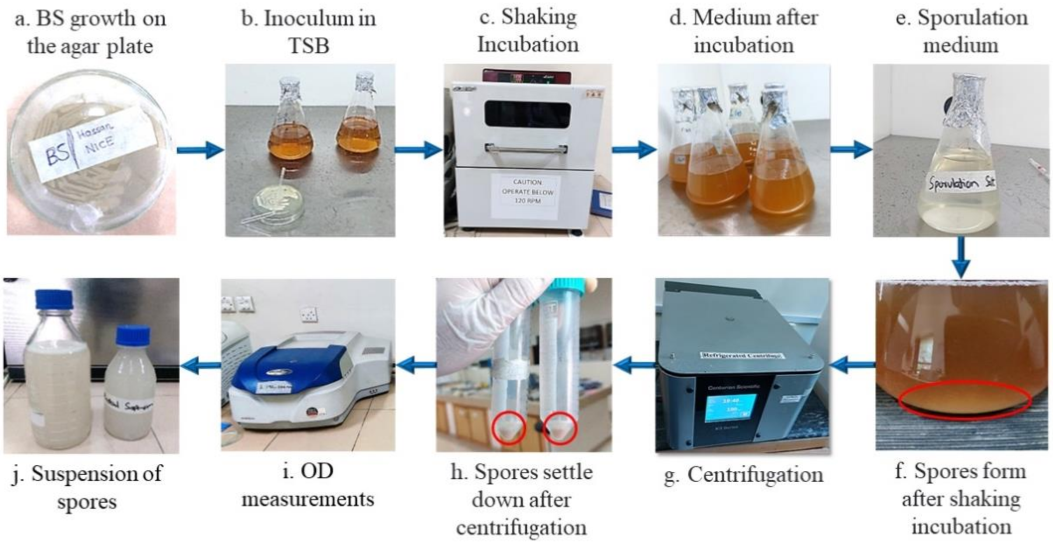

Figure 3-1 Preparation of bacterial spores

3.1.3 SF as an immobilization media

As SF was cut in 25 mm of optimal length as reported in the literature [10,28] for its utilization in the cementitious mix. Its absorption and adsorption capacity termed sorption capacity was measured according to the literature [10] to make sure that it can carry an adequate amount of BS. The properties of SF are presented in Table 3-3.

Thermal gravimetric analysis (TGA) and Fourier Transformed Infrared (FTIR) Spectroscopy were conducted to characterize the SF. TGA assessment was performed up to 600 ˚C at the increment of 1 ˚C/ min rise in temperature as shown in Figure 3-2 (b). Initially, up to 250 ˚C, mass loss of 12.2% is associated with the loss of intra and intermolecular water while from 251 to 400 ˚C, mass loss of 65.8% is linked with the fast degradation of cellulose and hemicellulose structure of SF. Beyond 401 ˚C, the mass loss decreases insignificantly due to the annealing of transformed char [111]. The

FTIR spectroscopy was performed in the 400–4000 cm^{-1} spectrum region as shown in Figure 3-2 (c). A sharp hump at 3328 cm^{-1} wave number is assigned to the O–H bond of the glycosidic bonds in cellulose [112]. A broad hump at 2915 cm^{-1} is associated with the C–H bonds of alkyl groups in aliphatic compounds of cellulose, lignin, and hemicellulose [113]. The carbonyl hump at 1731 cm^{-1} relates to C=O unconjugated bonding of the acetyl and ester groups of hemicelluloses [114]. CH_2 bonding present in cellulose resulted in a peak at 1423 cm^{-1} [113]. A broad hump at 1157, 1026, and 897 cm^{-1} has been linked with C-O-C and C–H bonding present in the pyranose ring structure of cellulose [115].

Table 3-3: Properties of SF

Sorption (%)	Diameter (mm)	Length (mm)	Density (g/cm^3)
186	0.06-0.24	25±5	1.5

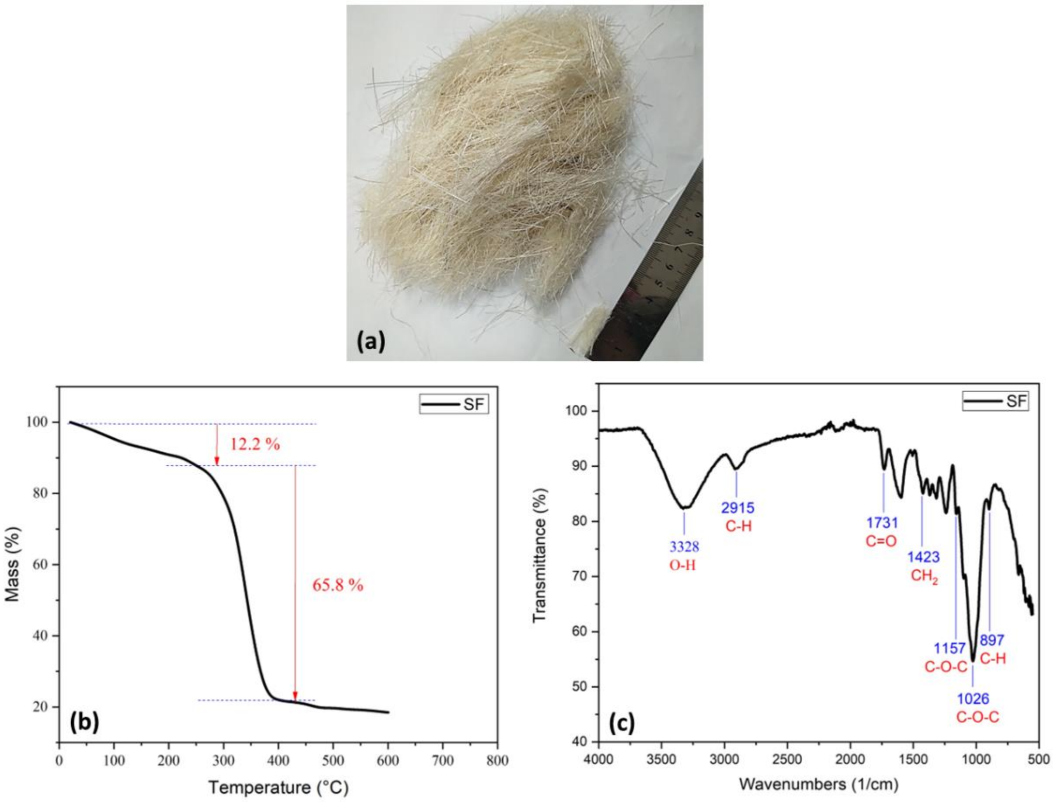

Figure 3-2. SF and its characterization (a) SF cut in 25 mm of optimal length (b) TGA plot and (c) FTIR spectrum of SF

3.2 Compatibility of BS with SF

Two methods were opted to confirm the compatibility of BS with SF. In the first method, SF was simply strewed on the fresh BS-streaked agar media plate after that 24 h incubation at 37 ˚C was done and its growth pattern was visually observed [3]. As shown in Figure 3-3 (a), SF does not hinder the growth pattern of BS confirming its compatibility. The second method is to make sure that SF does not result in the killing of bacterial spores and is capable to be used as a carrier media for BS in the longer run. FTIR of BS immobilized in SF (BISF) was carried out after 90 days to get the fingerprint spectra of inside microbial strains [116]. Figure 3-3 (b) is showing the FTIR spectra of BISF in the 400–4000 cm^{-1} spectrum region. Absorption of BS cell mass in SF resulted in an increase of broad hump at 3332 cm^{-1} which is because of the presence of NH_2 stretching in adenine, cytosine, quinine, and O–H stretching vibration [117]. The C–H stretching in the aliphatic of BS cell walls rises to the broad peak at 2918 cm^{-1} [118]. The addition of BS in SF resulted in new broad humps at 1642 cm^{-1}, 1536 cm^{-1} and 1243 cm^{-1} were linked with amide I, amide II, and amide III in a starving cell mass of BS [117]. A rise in peak at 1042 cm^{-1} is the result of additional polysaccharides due to BS cell mass [119]. The peak at 549 cm^{-1} is associated with phospholipids and RNA in BS [117]. This proves the ability of SF to be used as a carrier media for BS.

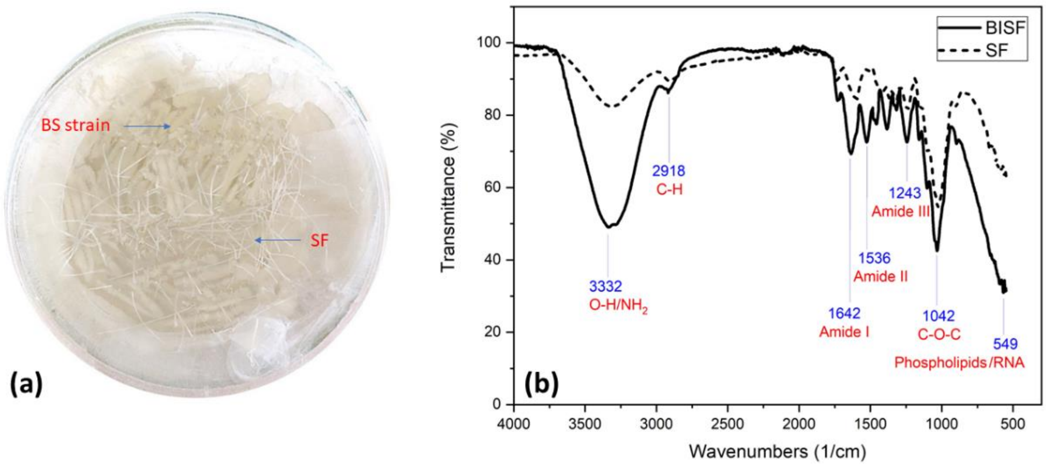

Figure 3-3 Compatibility of BS with SF (a) SF strewed on BS-streaked plate (b) FTIR of BISF

3.3 Mix proportions and specimen preparation

In this study, four different types of mixes were investigated designated as PCM, plain control mix; FCM, fiber control mix; PBM, plain bacterial mix; and FBM, fiber bacterial mix. In FCM and FBM, 1.0 % of SF by weight of cement was added considering the reported optimal performance at the mentioned dose for concrete [20,24,33]. In all the mixes a constant water-binder ratio of 0.45 was used. The slump was maintained in the range of 40-50 mm by controlling the dose of superplasticizer as practiced in the previous literature [21,26,28]. Calcium lactate used as a mineral precursor was also added in all mixes to have uniformity [3]. The details of mix proportions are shown in Table 3-4.

For each formulation firstly cement, fine and coarse aggregate were premixed for 1 min in a concrete mixer followed by wet mixing of formulated mixes. In PBM, the bacterial solution was incorporated directly as a replacement for mixing water; while in FBC, SF was soaked in the bacterial solution for 1 h before their mixing in concrete. In FCM and FBM to avoid clump formation and agglomeration effect, SF was slowly added to the mixer within 2 mins of wet mixing. Mixing was continued for another 1 min to obtain mix with a uniform fiber dispersion [17]. The prepared fresh concrete mix was poured into cylindrical molds (100 x 200 mm) and compacted with a vibrator. After 24 h of casting, the samples were demolded and then were water cured at 23± 2 ˚C until they reached the testing age.

Table 3-4: Mix Design of different mixes

Materials	PCM	FCM	PBM	FBM
Cement (kg/m^3)	392	392	392	392
Fine aggregate (kg/m^3)	863	863	863	863
Coarse aggregate (kg/m^3)	941	941	941	941
Water/cement ratio	0.45	0.45	0.45	0.45
Bacterial spores content (cell/cm^3)	0	0	6×10^8	6×10^8
Fiber (kg/m^3)	0	3.92	0	3.92
Superplasticizer (kg/m^3)	2.55	4.31	2.55	4.31
Calcium lactate (kg/m^3)	23.52	23.52	23.52	23.52

3.4 Testing procedure

The entire testing procedure was primarily branched into two phases. Initially, tests for investigating the compressive strength, split tensile strength, and sorptivity of different formulations were performed. Compressive strength and split tensile strength were determined according to ASTM C 39 [50] and ASTM C 496 [51] after 3, 14, and 28 days of curing. The sorptivity test was performed according to ASTM C 1585 [12] in which an increase in mass with respect to time is monitored by exposing one face of a test sample to water while remaining the other faces sealed with sealant. The second phase involved assessing self-healing efficacy in terms of crack healing, recovered compressive strength, and UPV improvement over two successive damage cycles. The visual inspection of cracks was done by pre-cracking the samples to their complete strength during each damage cycle. A lower loading rate of 0.1 MPa/sec had been employed during the pre-cracking to adequately monitor the cracks. Since the recovered properties after the complete strength were limited, these samples were employed for qualitative assessment of bio-crack healing. An optical microscope (HC-2950) of 0.02 mm least count was used for measuring the crack filling during the healing period. For the first and second healing cycles, the same duration of 28 days in water was adopted. Recovered compressive strength (RCS) and improvement in the ultrasonic pulse velocity (UPV) indirectly quantify healing proficiency. To investigate these, samples were damaged at 85% of their strength in the first damage cycle. To have stable crack growth and propagation during the second damage cycle, the specimens were damaged again at 85% of their recovered strength after the first healing cycle based on the quasi-linear constitutive stress-strain relationship for damaged concrete [52,53]. CSR at end of each healing cycle was estimated through Eq (1).

$$RCS\ (\%) = 1 - \frac{C_U - C_{AH}}{Cu} \times 100 \qquad (1)$$

Where:

C_u = ultimate compressive strength

C_{AH} = compressive strength after the healing cycle

The UPV test was conducted according to ASTM C 597 [54]. For improvement in UPV, ultrasonic pulse transmission time was initially recorded immediately after cracking, and later after 28 days of healing. UPV was computed as the ratio of the distance traveled by the wave to the time it has taken to propagate. Healing extent (HE) in terms of UPV for each healing cycle was estimated as the percentage difference between initial and final transmitted velocities. To investigate the microstructural changes due to microbial precipitation, Scanning Electron Microscope (SEM) and Energy Dispersive Spectroscopy (EDS) were employed for all four mixes. For conducting these tests, chunks of 1 cm^2 were extracted from the concrete near the cracks, then dried for 48 hours followed by gold plating, and finally examined at higher magnification. To monitor the structural fingerprint, and chemical modifications due to microbial precipitation; TGA, FTIR, and Raman Spectroscopy were performed on all the powdered cementitious mixes. TGA analysis was conducted up to 800 ˚C at the increment of 1 ˚C/ min rise in temperature. The FTIR spectroscopy was made in the 400-4000 cm^{-1} spectrum range while the Raman spectroscopy was conducted in the 100-1600 cm^{-1} spectrum range. The forensic diagnosis of the healing precipitate collected after the second healing cycle from the healed cracks of FBM samples was also performed. Additionally, XRD analysis was carried out for the morphological assessment of the healing product to determine its crystalline components and phase purity. The XRD analysis was performed at scanning angle 2-theta (2θ) ranging from 20°-80° with a step count of 0.02. Copper was employed as an x-ray target element because of its excellent thermal conductivity.

4 RESULTS AND DISCUSSIONS

4.1 Compressive strength test

The compressive strength of cementitious materials is a quantifiable measure of their performance. The compressive strengths of all four mixes at different ages of curing were determined according to standard ASTM C-39 [50] and are represented in Figure 4. (a). PCM showed a compressive strength of 14.01 MPa, 25.21 MPa, and 27.65 MPa at 3,14 and 28 days, respectively. In the case of FCM, an inappreciable improvement in compressive strength was depicted due to aided reinforcement by the fibers [49,55]. The percentage enhancement in compressive strength was found to be 1.14%, 2.32%, and 2.81% at 3, 14, and 28 days in FCM compared to PCM. Past studies have also reported that adding fibers to concrete has an insignificant effect on its compression strength [46,56,57]. Direct incorporation of BS into the concrete mix results in an appreciable enhancement in compressive strength. At 3, 14, and 28 days, the percentage strength improvement in PBM compared to PCM was 7.03%, 7.86%, and 8.14% respectively. This could be attributed to bio-synthesized $CaCO_3$ resulting in pore refinement of the concrete matrix and, in turn, increasing its load-taking ability [58,59]. FBM samples with SF as an immobilizer for BS attained a maximum compressive strength of 15.54, 27.90, and 31.51 MPa at 3, 14, and 28 days. At the mentioned intervals, the percentage increase compared to PCM is 10.88%, 10.65%, and 13.96% respectively. Thus, compared to other mixes FBM showed the maximum compressive strength, which can be attributed to the lamellar structure of SF that protects BS during mixing and casting. Consequently, increasing viable bacterial spores in the concrete; therefore greater bio-synthesized $CaCO_3$ precipitation and pore refinement can occur [14,60]. These findings are in accordance with the findings of Rauf et al. [10] that cellulosic fiber preserves the BS strains thereby significantly improving concrete compression strength. Thus, the addition of BS resulted in bio-synthesized $CaCO_3$ formation that densified the concrete microstructure as also shown in SEM micrographs and EDS results given in Figure 4-1 and Figure 4-2.

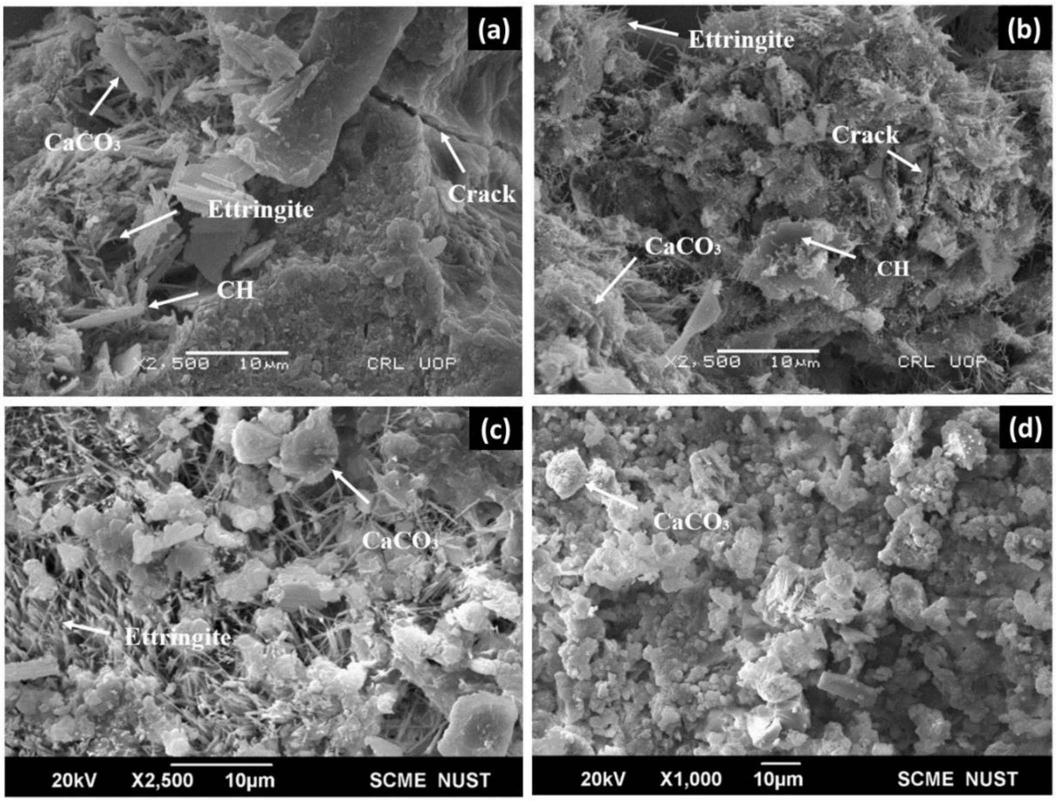

Figure 4-1. SEM images of the analyzed concrete samples

Compared to PCM and FCM in Figure 4-1(a) and Figure 4-1(b) copious amounts of $CaCO_3$ crystals in PBM and FBM were found as seen in Figure 4-1(c) and Figure 4-1(d). The biosynthesized $CaCO_3$ existed in the form of agglomerated rhombohedral crystals confirming it as calcite [10]. Results from EDS, as illustrated in Figure 4-2, also verify this as it is evident that the bacterial mixes have a comparatively high calcium content. Thus, enhanced compressive strength of the bacterial mixes was noticed due to calcite precipitation and pore refinement.

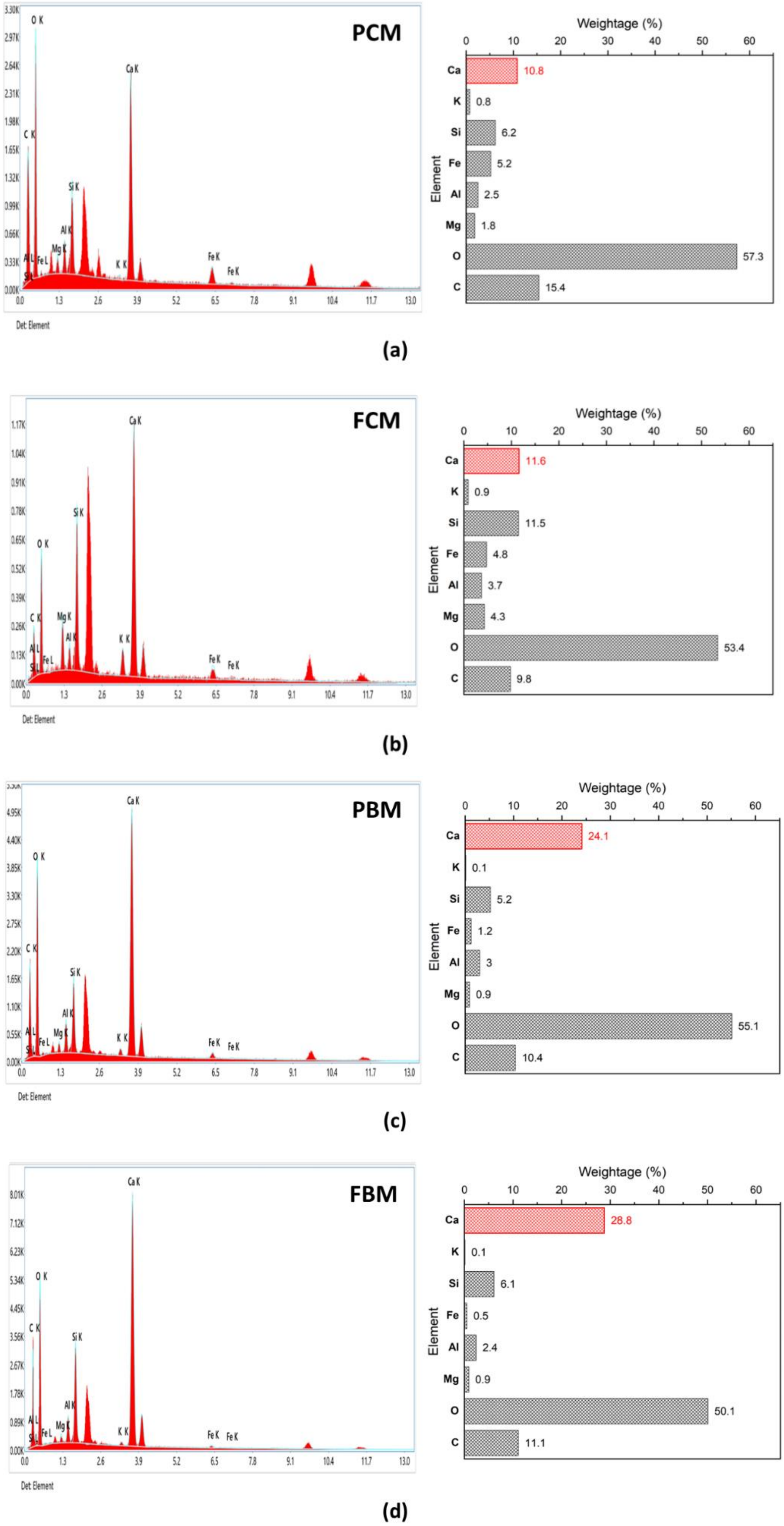

Figure 4-2. EDS analysis of the analyzed concrete samples

4.2 Split tensile strength test

Tensile strength is considered one of the important parameters to evaluate bond strength [16]. This test was carried out in accordance with ASTM-C496/ C496M guidelines [51]. Results of split tensile strength at different intervals of 3, 14, and 28 days are reported in Figure 4-3 (b). PCM mixes attained 1.53 MPa, 2.41 MPa, and 2.55 MPa of tensile strength at 3,14 and 28 days, respectively. Improvement in the tensile strength was quite noticeable upon the incorporation of SF and BS. However, FCM specimens showed significant enhancement in tensile strength compared to PBM. It could be attributed that in the case of split tension, the effect of fiber reinforcement is dominant as reported in the literature [46,56,57,61] The bio-synthesized $CaCO_3$ improved the interfacial bonding with adjacent cementitious matrix, therefore, enhancing tensile strength in PBM specimens [16]. In the case of FCM specimens, the percentage enhancement in tensile strength was found to be 11.71%, 15.79%, and 20.79% while in the case of PBM it was found to be 4.56%, 6.99%, and 8.11% at 3, 14, and 28 days respectively in comparison to PCM. A similar trend was reported for the FCM and PBM mixes in literature as well [55,59]. The FBM showed 25.41%, 29.75%, and 36.82% percentage improvement in tensile strength at 3, 14, and 28 days compared to PCM which is due to the symbiotic action of fiber reinforcement and bio-synthesized $CaCO_3$ [62]. Moreover, it was reported [63] that the inclusion of amines through immobilized bacterial spores as identified in the FTIR spectrum (Figure 3-3 (b)) results in surface modification of SF to establish a strong interfacial bond.

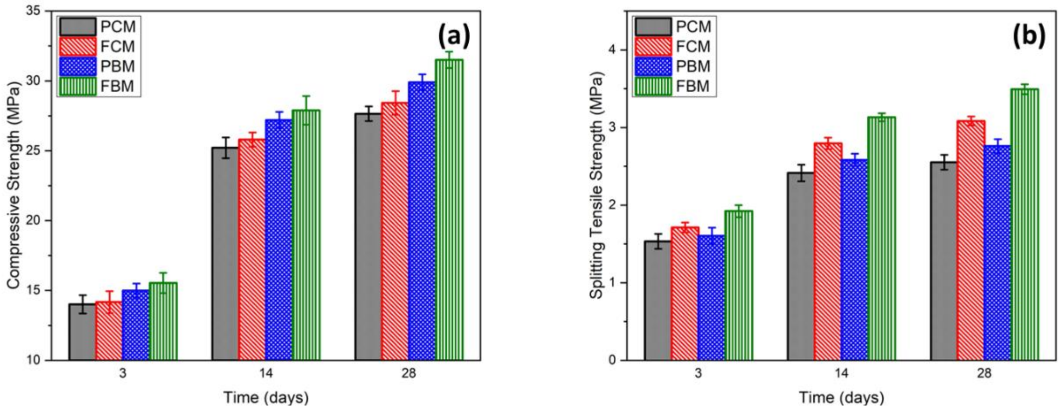

Figure 4-3. (a) Compressive strength (b) Splitting tensile strength of all mixes at different ages of curing

4.3 Sorptivity test

Figure 4-4 shows the sorptivity coefficient values obtained from the sorptivity test of the formulated concrete mixes. It has been found that the addition of SF marginally increased the water absorption rate as it can act as a water-conducting channel in the concrete mix, thereby increasing the capillary water absorption [64,65]. Previous studies have also found that fibers have no prominent effect on the water absorption capacity of concrete [35,61,65]. The sorption coefficient is decreased significantly with the incorporation of BS, which is attributed to densification and pore refinement of the concrete mix as a result of bio-mineralized $CaCO_3$ as also reported in the literature[23,66–68].

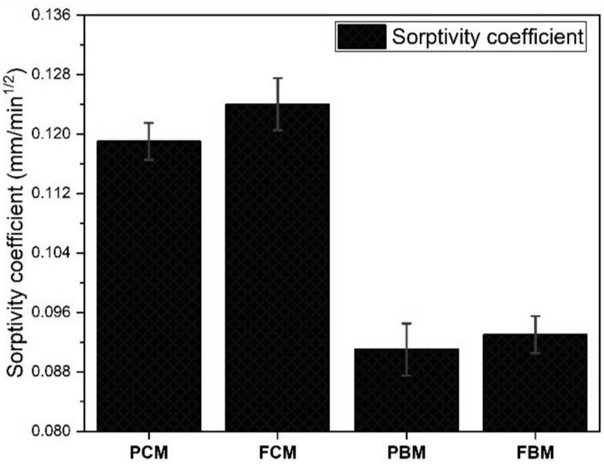

Figure 4-4. Sorptivity coefficient of all mixes

4.4 Self-healing investigations

4.4.1 Visual crack analysis

In the self-healing investigations, the first step includes visual analysis of crack widths healed due to bio-synthesized $CaCO_3$ using a crack width measuring microscope. Healing during each cycle is measured as the difference between the width of the crack immediately after pre-cracking and the subsequent 28th-day healing period. Figure 4-5 depicts the healing of cracks for all four mixes after two healing cycles.

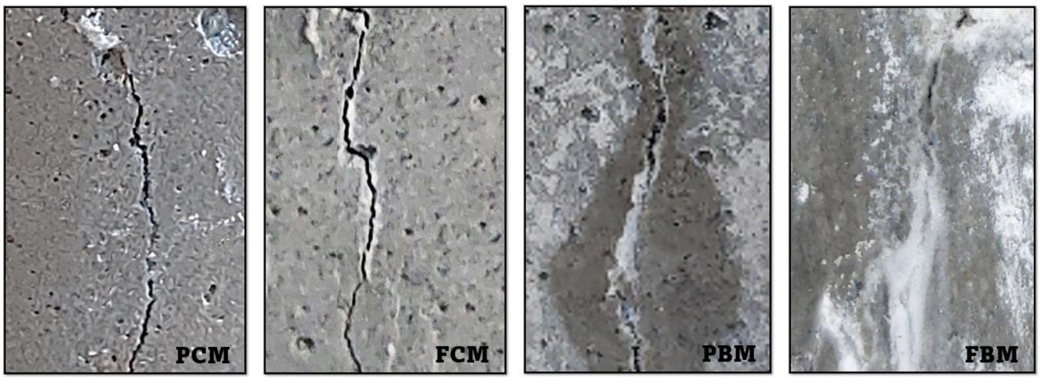

Figure 4-5. Crack healing in different mixes

The data of average crack-width healed in two successive damage cycles for all the formulations is presented in

Table 4-1. In PCM and FCM control mixes, healing occurs as a result of autogenous healing which is attributed to un-hydrated cement particles interacting in the presence of moisture after cracking, clogging of cracks by detached loose particles, or $CaCO_3$ formation due to interaction of $Ca(OH)_2$ with dissolved CO_2 in water [8,10]. A sharp decrease in healing is found during the second healing cycle where it shows that the repair of concrete cracks is insignificant.

In PBM and FBM specimens, significant enhancement in crack healing up to 0.48 mm and 0.37 mm was noticed as the addition of BS catalyzes the synthesis of $CaCO_3$ crystals [2,3,18,20]. Since the PBM does not contain any protective media for BS, therefore comparatively less healing was found than that of FBM. The densification and direct exposure to a highly alkaline environment of concrete matrix reduce the viability of directly intruded BS [14,69]. During the second healing cycle, PBM and FBM specimens showed 0.15 mm and 0.28 mm of surficial healing. It was found that healing occurs even during the second healing cycle, however, a drop has been observed likely due to a reduction in the availability of healing agents consumed during the first healing cycle. Long-span viability of Bacillus pseudofirmus bacterial spores till 4 months duration has been established through literature as well [13]. The limited strains of BS in crack proximity and its readily transport in the cracks could be responsible for healing during the second cycle [19]. The improved crack healing in two healing cycles of FBM is attributed to the immobilization technique that effectively preserves bacteria for a relatively longer duration in concrete [20,70]. These findings are in agreement with those of Rauf et al., who investigated the potential of coir, flax, and jute fibers as immobilizers [10].

Table 4-1: Average crack-width (mm) healed in two successive healing phases

Formulation	First Healing Cycle	Second Healing Cycle
PCM	0.15	0.05
FCM	0.16	0.05
PBM	0.37	0.15
FBM	0.48	0.28

4.4.2 Compressive strength recovery

The damaging process also induces internal micro-cracks in the concrete specimens which have a detrimental impact on its strength [71]. These damaged specimens can recover their strength over time through self-healing mechanisms. Therefore, healing proficiency was quantified in terms of percentage RCS. The results of RCS are presented in Figure 4-6. With the increase in pre-cracking age, a decrease in RCS was noticed in two successive healing cycles. This is credited to progressive hydration reactions with time, depleting autogenous and autonomous healing thereby limiting the self-healing adequacy [72].

During the first healing cycle maximum, RCS up to 66.38 % was noticed in PCM specimens. Although due to the fiber reinforcement effect, FCM specimens achieved higher RCS up to 71.62 %, however, it was still lower due to only autogenous healing [70,73]. Despite no immobilizer in PBM, a better RCS of up to 75.73 % was attained during the first healing cycle attributed to the combined effect of autogenous and autonomous healing. However, the contribution from autonomous healing through bacterial spores was limited due to their survival challenges on direct incorporation into concrete [18]. The immobilization technique successfully preserved BS, which resulted in the relatively improved performance of FBM owing to better RCS of up to 82.65 %. Similar findings were found by Vijay & Murmu [21], who reported that RCS was high in bacterial concrete and bacterial concrete with basalt fibers in comparison to its plain and fiber control specimens. Due to the reduction in autogenous and autonomous healing and increase in damage level, a sharp drop in RCS was observed during the second healing cycle in all the formulated mixtures. In the second healing cycle, PCM specimens exhibited the least RCS up to 35.34 %. FCM specimens unlike in the first healing cycle showed relatively better RCS than PBM during the second healing cycle. This is due to its fiber reinforcement effect that became significant as the extent of damage increased under repeated stress cycles [74]. These findings are consistent with the findings of Ali et al. [35] who investigated PP and banana stem fibers in concrete. He concluded that fiber addition had no significant effect on compressive strength after the first damaging cycle, while it became quite noticeable in the case of the second damaging cycle. A maximum of 42.66 % and 39.10 % of RCS was observed in FCM and PBM specimens after the second healing cycle. Further, the damage induced during the second loading cycle in FCM specimens was believed to be on the lower side in terms of crack opening due to the development of multiple discrete cracks by bridging fibers curable through autogenous healing [20,75,76]. Compared to PCM, PBM exhibited better RCS due to limited $CaCO_3$ precipitation by survived bacteria inducing autonomous healing. Immobilization of bacterial spores along with aided confinement provided by fibers resulted in considerably improved performance of FBM specimens showing a maximum of 50.42 % of RCS during the second healing cycle. These findings affirmed the bio-compatibility of SF with BS resulting in improved healing proficiency via bio-mineralization in two successive damage cycles.

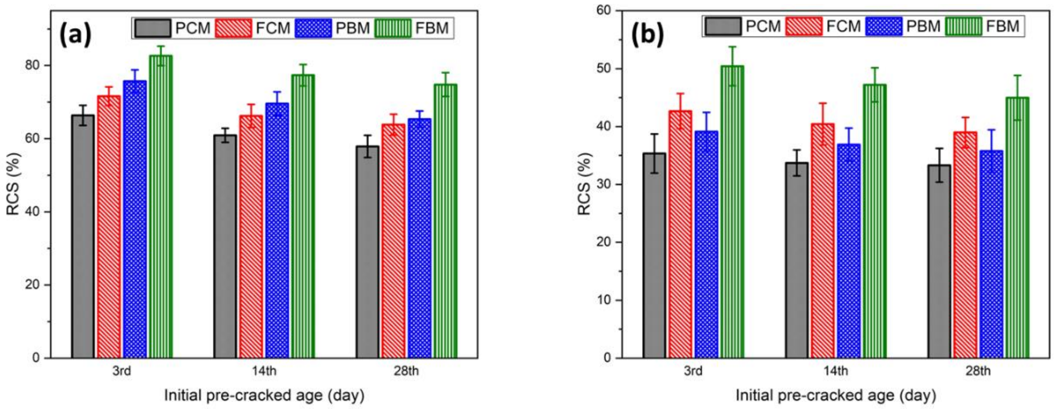

Figure 4-6. (a) Recovered compressive strength (RCS) after the first and (b) second healing cycle

4.4.3 Improvement in UPV

When cracks form, the transmission time of ultrasonic waves increases as it passes through the cracked concrete. Due to the persistent autogenous and autonomous healing, gradual filling of micro-cracks and pores occurs which, reduces the transmission time of ultrasonic pulse waves [10]. To investigate the healing extent of internal microcracks because of self-healing in damaged samples, the percentage improvements in UPV termed HE was also computed. These results corresponding to each formulated mix are shown in Figure 4-7.

From the data obtained after both healing cycles, it is clear that with the increase in pre-cracking age HE decreases which is due to an increase in the degree of hydration of concrete thereby limiting both autogenous and autonomous healing [77]. During the first and second healing cycles, a maximum of 12.46 % and 3.10 % of HE was attained in PCM specimens while FCM specimens attained a maximum of 14.39 % and 3.61 % of HE. The HE in the PCM sample was found to be the least of all the samples after both healing cycles. In FCM, HE was comparatively enhanced due to relatively small cracks developed during pre-cracking as reported in the literature [20,73]. A maximum of 23.87 and 9.39 of HE (%) during the first and second healing cycles was attained in PBM specimens respectively. The substantial improvement in HE of PBM specimens is due to the stimulated healing mechanism by microbes filling the internal micro-cracks and densifying the concrete microstructure. FBM specimens showed the highest amount of self-healing with a maximum of 29.02 and 13.58 of HE (%) recorded during the first and second healing cycles. The higher HE of FBM in two successive healing cycles endorses the effectiveness of SF in conserving BS which, resulted in ample production of bio-mediated calcite. These findings are in line with previous investigations [10,12,78,79].

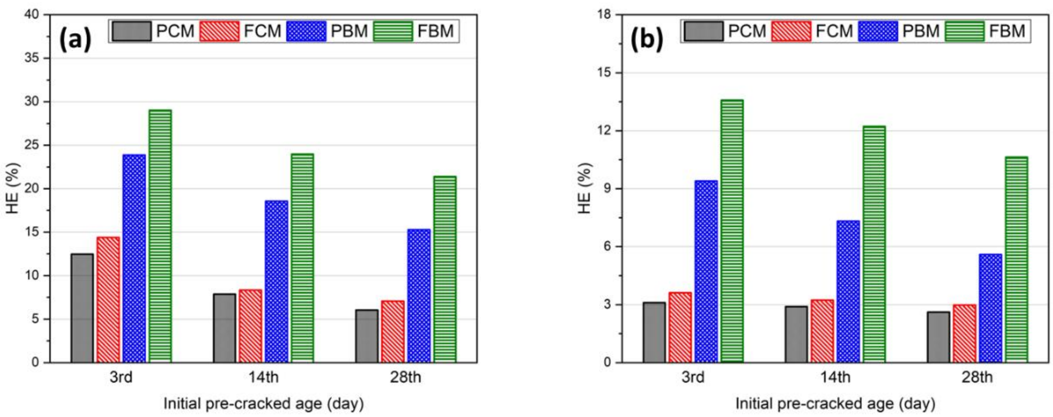

Figure 4-7. (a) Healing Extent (%) in terms of improvement in UPV after the first and (b) second healing cycle

4.4.4 Forensic Investigation

For forensic endorsement, Scanning Electron Microscope (SEM), Energy Dispersive Spectroscopy (EDS), X-ray diffraction (XRD), TGA, FTIR, and Raman Spectroscopy were employed to investigate the microstructure, morphology, and chemical modifications of microbial precipitation.

4.4.4.1 Scanning Electron Microscopy (SEM)

SEM of the bio-synthesized $CaCO_3$ was performed to investigate its microstructural analysis as presented respectively in Figure 4-8. The $CaCO_3$ may be found in form of calcite, aragonite, and vaterite polymorphs in bio-concrete. However, aragonite and vaterite are thermodynamically unstable and change to a stable form i.e., calcite [3,17,60]. The $CaCO_3$ precipitates owe lamellar rhombohedral appearance confirming that healing precipitation was calcite [14,20]. Spherical and ellipsoidal shape bacterial spores of 0.08-0.8 μm are also visible in Figure 4-8, confirming the healing precipitation was a result of the metabolic activity of BS [8].

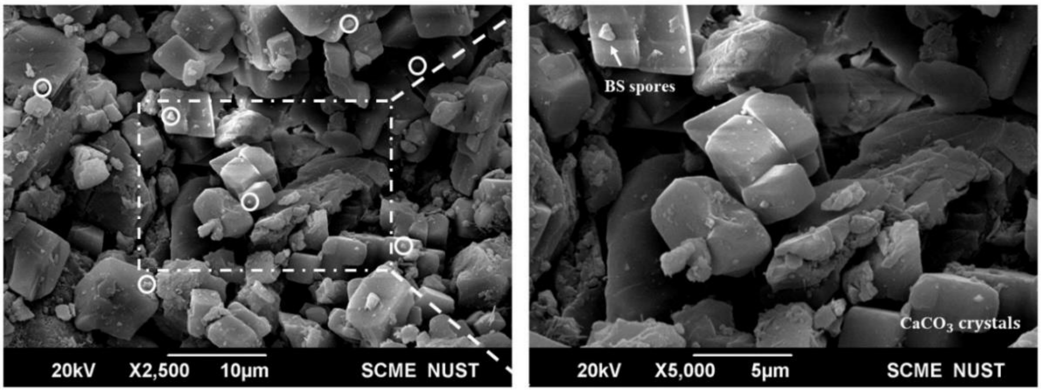

Figure 4-8. SEM of bio-synthesized healing precipitation collected from cracks

4.4.4.2 Energy dispersive spectroscopy

EDS analysis of the precipitated healing product was performed to determine its composition as shown respectively in Figure 4-9. The existence of Ca, O, and C affirms the existence of $CaCO_3$ as the primary constituent of the healing precipitate [18]. The EDS analysis also shows the presence of Si and Mg elements in trace amounts. This proves that calcite was formed as a result of bacterial activity.

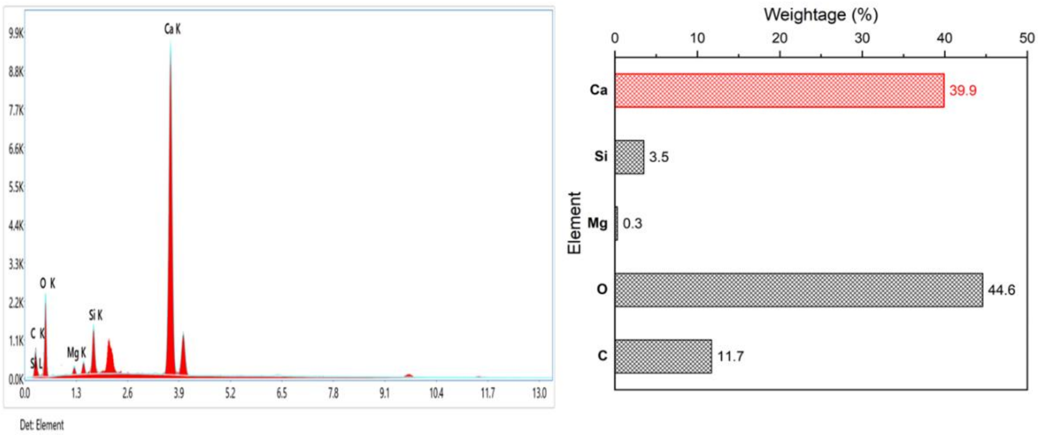

Figure 4-9. EDS analysis of bio-synthesized healing precipitate collected from cracks

4.4.4.3 Thermogravimetric Analysis (TGA)

This test is used to monitor the thermal degradation of a material with respect to an increase in temperature. As the chemical disintegrations of a particular compound lie in a particular temperature range, therefore TGA can be used to quantify the percentage of a particular compound in a material. TGA of both the powdered cementitious mix and healing precipitate was performed.

TGA of the powdered cementitious mix was performed to manifest the bio-synthesized $CaCO_3$. Based on chemical disintegrations, the weight loss regions were divided into three ranges, the same is endorsed by literature. The first thermal degradation range is 100-400 ˚C wherein CSH gels and ettringite losses adsorbed water and subsequently dissociate [80]. The second range of weight loss between 400-600 ˚C records the disintegration of $Ca(OH)_2$ as provided in Eq (2.2) [60,69]. Whereas, the decomposition of $CaCO_3$ occurs in the third range of 600-800 ˚C [3,18]. The reaction is given in Eq (2.2).

$$Ca(OH)_2 \rightarrow CaO + H_2O \tag{2}$$

$$CaCO_3 \rightarrow CaO + CO_2 \tag{3}$$

The mass loss due to $CaCO_3$ disintegration in different mixes is given in Table 4-2. PCM and FCM showed 3.762% and 3.802% mass loss due to $CaCO_3$ disintegration, implying low proportions of precipitated $CaCO_3$. The bacterial mixes depicted relatively greater mass loss due to $CaCO_3$ disintegration. This is primarily due to microbial synthesis of $CaCO_3$ in addition to any conceivable carbonation [75]. PBM having directly intruded microbes depicted mass loss of 4.745% due to $CaCO_3$ disintegration. FBM mix showed a significantly higher mass loss of 6.231% due to $CaCO_3$ disintegration, this indicates the efficacy of the SF as an immobilizer in preserving the pro-longed microbial activity of BS.

The healing precipitation was subjected to TGA analysis as shown in Figure 4-10 (b) for $CaCO_3$ affirmation. An intense loss in mass of about 29.8% from 600 to 800 ˚C is due to the disintegration of $CaCO_3$ [3,18]. This endorses that healing precipitation was $CaCO_3$.

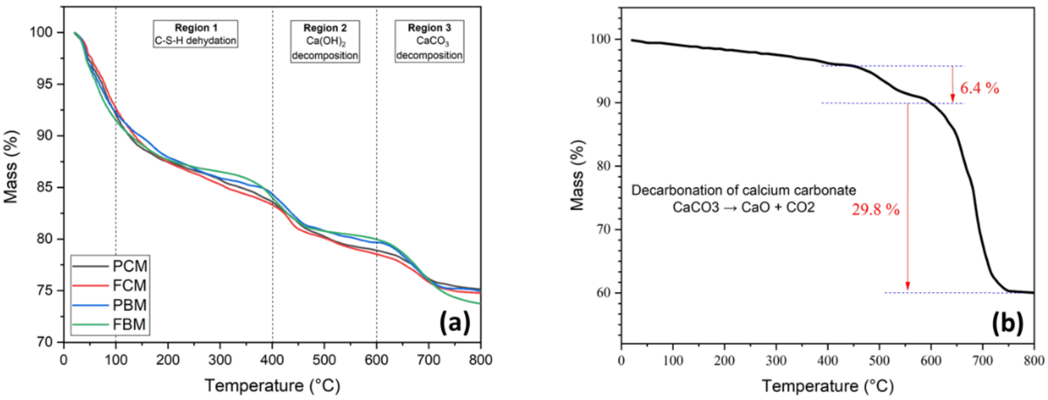

Figure 4-10. (a) Thermographs of the analyzed concrete mixes and (b) bio-synthesized healing precipitation

Table 4-2 Mass loss due to $CaCO_3$ disintegration (600-800 ˚C) in different mixes

Sample	Δ m %
PCM	3.762
FCM	3.802
PBM	4.745
FBM	6.231

4.4.4.4 X-ray diffraction (XRD) analysis

Diffraction patterns of the precipitated healing powders cautiously scratched out from healed cracks and investigated through X'Pert HighScore are presented in Figure 4-11. Both autogenous and autonomous healing results in $CaCO_3$ precipitation [10]. The diffractogram of all the healing precipitates showed a peak at 2θ=29˚-30˚ indicating the presence of $CaCO_3$. PBM and FBM samples showed an intense sharp peak which indicates highly crystalline structures of $CaCO_3$ [17]. This confirms that calcite was formed due to bacterial activity. Traces of some other minerals were identified and are also shown in Figure 14.

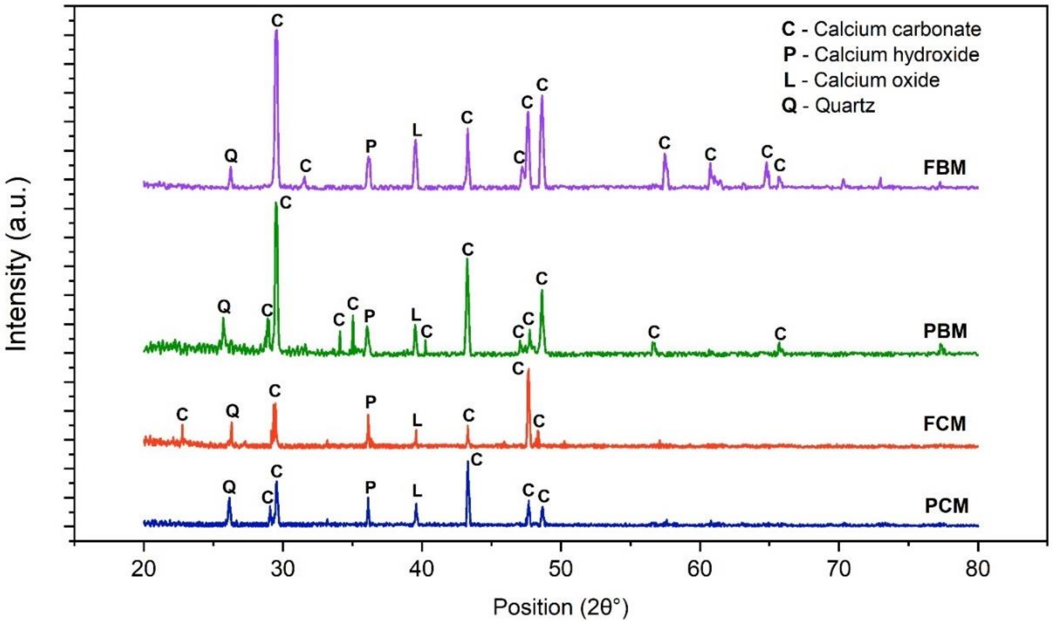

Figure 4-11. X-ray Diffractograms of healing precipitation

4.4.4.5 Fourier Transformed Infrared (FTIR) Spectroscopy

The intensity of absorption bands of high energy infrared frequencies by chemical bonds of the crystalline phases at their natural frequency can be used to characterize it. Figure 4-12 (a) shows the results of FTIR of the powdered cementitious mix while Figure 15 (b) represents the FTIR spectrum of healing precipitation.

FTIR graph of the powdered cementitious mix identified the hydration phases and crystalline changes due to self-healing as shown in Figure 4-12 (a). The stretching vibration of O-H in portlandite centered peak at around 3429 cm^{-1} [80]. A small hump observed at around 1644 cm^{-1} relates to H-OH and C-H bending in the calcium silicate hydrate (C-S-H) gel [81,82]. Si-O stretching in the C-S-H phase results in peaks at around 1078 and 977 cm^{-1} [83]. The peak at around 1409, 874, and 712 cm^{-1} might be associated with asymmetric stretching, out-of-plan bending, and planar bending vibrations of C-O of carbonates formed due to the self-healing mechanism [2,82]. The spectrum of bacterial mixes i.e., PBM and FBM showed intense peaks linked with carbonates thereby implying bio-synthesis of $CaCO_3$ [84].

The FTIR spectrum of the healing precipitation is shown in Figure 4-12 (b). The principal vibrational bands for calcite are therefore recognized in healing precipitation confirming it as bio-synthesized calcite [2]. The occurrence of small humps could be due to hydrous and anhydrous cement phases.

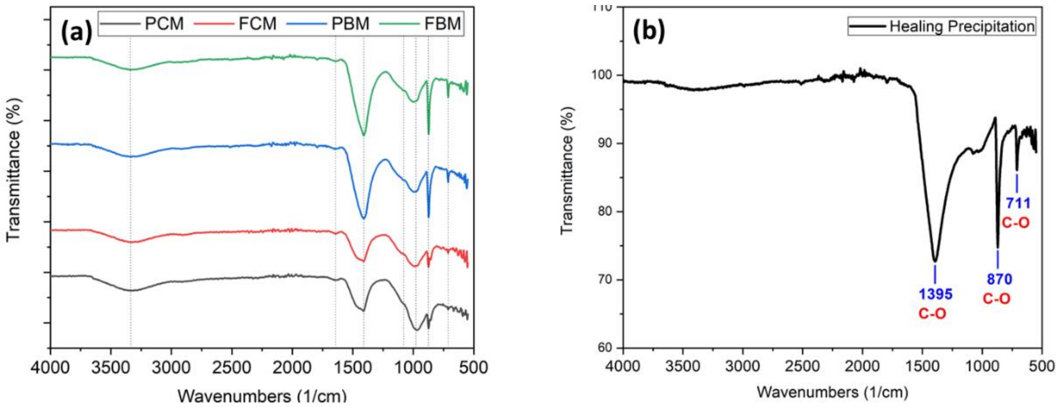

Figure 4-12. (a) FTIR spectrum of the analyzed concrete mixes and (b) bio-synthesized healing precipitation

4.4.4.6 Raman Spectroscopy

Figure 4-13 (a) depicts the experimental results of the Raman spectroscopy for all four mixes. The Ca–O vibration of portlandite produced due to the hydration process might be responsible for the peak at around 361 cm^{-1} [85]. Peaks at around 463, 646, 845, and 987 cm^{-1} are associated with SiO_4^{-2} of calcium silicate hydrate (CSH). A broad hump at around 1086 cm^{-1} is due to CO_3^{-2} in $CaCO_3$ [85–87]. The spectrum of bacterial mixes i.e., PBM and FBM showed the strongest CO_3^{-2} peak indicating the highest degree of $CaCO_3$ crystallization occurred due to microbial action [3,88].

Figure 4-13 (b) showed the Raman spectra of the healing precipitation. The characteristic peak at around 1091 cm^{-1} corresponds to the symmetric stretching mode of the CO_3^{-2} in $CaCO_3$ [89]. The in-plane bending in CO_3^{-2} results in a peak at around 718 cm^{-1} [90]. As the healing precipitation was collected from the cracks, the occurrence of a small hump at around 470 cm^{-1} could be due to Si–O–Si stretching vibrations of the hydration product. Peaks at around 287 cm^{-1} and 154 cm^{-1} correspond to lattice vibrations [91]. The peaks in the Raman spectrum were observed to be derived from rhombohedral calcite crystals validating the healing product as bio-synthesized calcite [92].

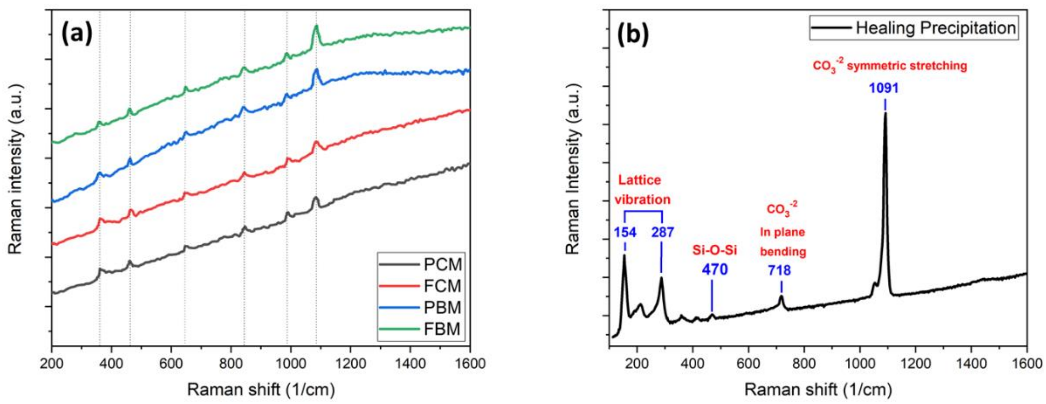

Figure 4-13. (a) Raman spectrum of the analyzed concrete mixes and (b) bio-synthesized healing precipitate

5 CONCLUSIONS AND RECOMMENDATIONS

In the current study, the potential of SF as a suitable immobilizer for BS was investigated in bio-based self-healing concrete. The healing adequacy was investigated in two successive damage cycles. The following conclusions are drawn based on the experimental investigations:

- BS immobilized with SF exhibited the highest tensile and compressive strength yielding a maximum of 36.82% and 13.96% improvement in tensile and compressive strength compared to PCM. The intrusion of BS decreases the sorption capacity of concrete and confirms the densification and pore refinement of the concrete mix.
- The synergetic action of BS and SF contributes to better recovery of properties of the healed specimens with 82.65% and 50.42% regain in compressive strength and healing extent of 29.02% and 13.58% accessed through UPV testing after the first and second healing cycles.
- Immobilization of BS with SF successfully sustains its long-term viability contributing to 0.48 mm and 0.28 mm of average crack healing in the FBM mix while PBM displays 0.37 mm and 0.15 mm after the first and second healing cycles.
- Rhombohedral crystalline products in the agglomerated form found in the concrete microstructure affirm the formation of thermally stable calcium carbonate formed due to biomineralization. Moreover, EDS, TGA, FTIR, and Raman spectroscopy also endorse the formation of biosynthesized calcite.
- Consequently, SF can be considered as the potential immobilizer for the development of robust bio-concrete resilient to multiple damage cycles.

The following are recommendations for further study:

- The study should be extended to also include the various immobilizers for microbes.
- The investigation should be extended to include more repeated damage and healing cycles.
- The X-ray chromatography technique scan technique should be employed to examine the healing efficacy of bacterial-based self-healing concrete.

6 REFERENCES

[1] N. Shaheen, R.A. Khushnood, W. Khaliq, H. Murtaza, R. Iqbal, M.H. Khan, Synthesis and characterization of bio-immobilized nano/micro inert and reactive additives for feasibility investigation in self-healing concrete, Constr. Build. Mater. 226 (2019) 492–506. https://doi.org/10.1016/j.conbuildmat.2019.07.202.

[2] R.A. Khushnood, Z.A. Qureshi, N. Shaheen, S. Ali, Bio-mineralized self-healing recycled aggregate concrete for sustainable infrastructure, Sci. Total Environ. 703 (2020) 135007. https://doi.org/10.1016/j.scitotenv.2019.135007.

[3] M. Kanwal, R.A. Khushnood, W. Khaliq, A.G. Wattoo, T. Shahid, Synthesis of pyrolytic carbonized bagasse to immobilize Bacillus subtilis; application in healing micro-cracks and fracture properties of concrete, Cem. Concr. Compos. 126 (2022) 104334. https://doi.org/10.1016/j.cemconcomp.2021.104334.

[4] J. Xu, Y. Tang, X. Wang, Z. Wang, W. Yao, Application of ureolysis-based microbial CaCO3 precipitation in self-healing of concrete and inhibition of reinforcement corrosion, Constr. Build. Mater. 265 (2020) 120364. https://doi.org/10.1016/j.conbuildmat.2020.120364.

[5] S. Gupta, H.W. Kua, S.D. Pang, Healing cement mortar by immobilization of bacteria in biochar: An integrated approach of self-healing and carbon sequestration, Cem. Concr. Compos. 86 (2018) 238–254. https://doi.org/10.1016/j.cemconcomp.2017.11.015.

[6] H.W. Kua, S. Gupta, A.N. Aday, W. V. Srubar, Biochar-immobilized bacteria and superabsorbent polymers enable self-healing of fiber-reinforced concrete after multiple damage cycles, Cem. Concr. Compos. 100 (2019) 35–52. https://doi.org/10.1016/j.cemconcomp.2019.03.017.

[7] V. Wiktor, H.M. Jonkers, Quantification of crack-healing in novel bacteria-based self-healing concrete, Cem. Concr. Compos. 33 (2011) 763–770. https://doi.org/10.1016/j.cemconcomp.2011.03.012.

[8] A. Danish, M.A. Mosaberpanah, M.U. Salim, Past and present techniques of self-healing in cementitious materials: A critical review on efficiency of implemented treatments, J. Mater. Res. Technol. 9 (2020) 6883–6899. https://doi.org/10.1016/j.jmrt.2020.04.053.

[9] L.A. Le, G.D. Nguyen, H.H. Bui, A.H. Sheikh, A. Kotousov, Incorporation of

micro-cracking and fiber bridging mechanisms in constitutive modelling of fiber reinforced concrete, J. Mech. Phys. Solids. 133 (2019). https://doi.org/10.1016/j.jmps.2019.103732.

[10] M. Rauf, W. Khaliq, R.A. Khushnood, I. Ahmed, Comparative performance of different bacteria immobilized in natural fibers for self-healing in concrete, Constr. Build. Mater. 258 (2020) 119578. https://doi.org/10.1016/j.conbuildmat.2020.119578.

[11] H. Singh, R. Gupta, Influence of cellulose fiber addition on self-healing and water permeability of concrete, Case Stud. Constr. Mater. 12 (2020). https://doi.org/10.1016/j.cscm.2019.e00324.

[12] J. Zhang, Y. Liu, T. Feng, M. Zhou, L. Zhao, A. Zhou, Z. Li, Immobilizing bacteria in expanded perlite for the crack self-healing in concrete, Constr. Build. Mater. 148 (2017) 610–617. https://doi.org/10.1016/j.conbuildmat.2017.05.021.

[13] D. Snoeck, N. De Belie, Repeated Autogenous Healing in Strain-Hardening Cementitious Composites by Using Superabsorbent Polymers, J. Mater. Civ. Eng. 28 (2016) 04015086. https://doi.org/10.1061/(asce)mt.1943-5533.0001360.

[14] H. Amer Algaifi, S. Abu Bakar, A. Rahman Mohd. Sam, M. Ismail, A. Razin Zainal Abidin, S. Shahir, W. Ali Hamood Altowayti, Insight into the role of microbial calcium carbonate and the factors involved in self-healing concrete, Constr. Build. Mater. 254 (2020) 119258. https://doi.org/10.1016/j.conbuildmat.2020.119258.

[15] B. Saleem, A. Hussain, A. Khattak, A. Khan, Performance evaluation of bacterial self-healing rigid pavement by incorporating recycled brick aggregate, Cem. Concr. Compos. 117 (2021) 103914. https://doi.org/10.1016/j.cemconcomp.2020.103914.

[16] W. Khaliq, M.B. Ehsan, Crack healing in concrete using various bio influenced self-healing techniques, Constr. Build. Mater. 102 (2016) 349–357. https://doi.org/10.1016/j.conbuildmat.2015.11.006.

[17] G. Ren, B. Yao, H. Huang, X. Gao, Influence of Ss on the mechanical performance of ultra-high performance concretes, Constr. Build. Mater. 286 (2021) 122958. https://doi.org/10.1016/j.conbuildmat.2021.122958.

[18] S.R. Naraganti, R.M.R. Pannem, J. Putta, Impact resistance of hybrid fiber reinforced concrete containing sisal fibers, Ain Shams Eng. J. 10 (2019) 297–

305. https://doi.org/10.1016/j.asej.2018.12.004.

[19] G. Ren, X. Gao, H. Zhang, Utilization of hybrid sisal and steel fibers to improve elevated temperature resistance of ultra-high performance concrete, Cem. Concr. Compos. 130 (2022) 104555. https://doi.org/10.1016/j.cemconcomp.2022.104555.

[20] J. Ahmad, Z. Zhou, Mechanical Properties of Natural as well as Synthetic Fiber Reinforced Concrete: A Review, Constr. Build. Mater. 333 (2022) 127353. https://doi.org/10.1016/j.conbuildmat.2022.127353.

[21] L. Wang, T. He, Y. Zhou, S. Tang, J. Tan, Z. Liu, J. Su, The influence of fiber type and length on the cracking resistance, durability and pore structure of face slab concrete, Constr. Build. Mater. 282 (2021) 122706. https://doi.org/10.1016/j.conbuildmat.2021.122706.

[22] D. Zheng, W. Song, J. Fu, G. Xue, J. Li, S. Cao, Research on mechanical characteristics, fractal dimension and internal structure of fiber reinforced concrete under uniaxial compression, Constr. Build. Mater. 258 (2020) 120351. https://doi.org/10.1016/j.conbuildmat.2020.120351.

[23] B. Ali, L.A. Qureshi, Influence of glass fibers on mechanical and durability performance of concrete with recycled aggregates, Constr. Build. Mater. 228 (2019) 116783. https://doi.org/10.1016/j.conbuildmat.2019.116783.

[24] I. Shah, J. Li, S. Yang, Y. Zhang, A. Anwar, Experimental Investigation on the Mechanical Properties of Natural Fiber Reinforced Concrete, J. Renew. Mater. 10 (2022) 1307–1320. https://doi.org/10.32604/jrm.2022.017513.

[25] S. Rai P., H. N., K. D.V., S. Unnikrishnan, C. A., Mechanical strength and water penetration depth of palmyra fiber reinforced concrete, Mater. Today Proc. (2022). https://doi.org/10.1016/j.matpr.2022.05.049.

[26] S.H.A. Shah, M.T. Amir, B. Ali, M.H. El Ouni, Mechanical performance and environmental impact of normal strength concrete incorporating various levels of coconut fiber and recycled aggregates, Environ. Sci. Pollut. Res. (2022). https://doi.org/10.1007/s11356-022-21608-w.

[27] M. Ramli, W.H. Kwan, N.F. Abas, Strength and durability of coconut-fiber-reinforced concrete in aggressive environments, Constr. Build. Mater. 38 (2013) 554–566. https://doi.org/10.1016/j.conbuildmat.2012.09.002.

[28] B. Ali, M. Azab, H. Ahmed, R. Kurda, M. Hechmi, E. Ouni, A.B. Elhag, f, J. Build. Eng. (2022) 105024. https://doi.org/10.1016/j.jobe.2022.105024.

[29] M.L.M. Broeren, S.N.C. Dellaert, B. Cok, M.K. Patel, E. Worrell, L. Shen, Life cycle assessment of sisal fiber – Exploring how local practices can influence environmental performance, J. Clean. Prod. 149 (2017) 818–827. https://doi.org/10.1016/j.jclepro.2017.02.073.

[30] F.T. Raya, M.P. Marone, L.M. Carvalho, S.C. Rabelo, M.S. de Paula, M.F.Z. Campanari, L. Freschi, J.L.S. Mayer, O.R.R.F. Silva, P. Mieczkowski, M.F. Carazzolle, G.A.G. Pereira, Extreme physiology: Biomass and transcriptional profiling of three abandoned Agave cultivars, Ind. Crops Prod. 172 (2021). https://doi.org/10.1016/j.indcrop.2021.114043.

[31] FAO - Food and Agricultural Organization of the United Nations, Jute, Kenaf, Sisal, Abaca, Coir and Allied Fibers Statistical Bulletin 2020, Food Agric. Organ. United Nations. (2022) 1–43.

[32] A. Karimah, M.R. Ridho, S.S. Munawar, D.S. Adi, Ismadi, R. Damayanti, B. Subiyanto, W. Fatriasari, A. Fudholi, A review on natural fibers for development of eco-friendly bio-composite: characteristics, and utilizations, J. Mater. Res. Technol. 13 (2021) 2442–2458. https://doi.org/10.1016/j.jmrt.2021.06.014.

[33] R. Abirami, S.P. Sangeetha, K. Nadeemmishab, P.Y. Vaseem, K.S. Sad, Experimental behaviour of sisal and kenaf fiber reinforced concrete, AIP Conf. Proc. 2271 (2020). https://doi.org/10.1063/5.0024771.

[34] A.A. Okeola, S.O. Abuodha, J. Mwero, Experimental investigation of the physical and mechanical properties of sisal fiber-reinforced concrete, Fibers. 6 (2018). https://doi.org/10.3390/fib6030053.

[35] K. V. Sabarish, P. Paul, Bhuvaneshwari, J. Jones, An experimental investigation on properties of sisal fiber used in the concrete, Mater. Today Proc. 22 (2020) 439–443. https://doi.org/10.1016/j.matpr.2019.07.686.

[36] H. Singh, R. Gupta, Cellulose fiber as bacteria-carrier in mortar: Self-healing quantification using UPV, J. Build. Eng. 28 (2020) 101090. https://doi.org/10.1016/j.jobe.2019.101090.

[37] K. van Breugel, IS THERE A MARKET FOR SELF-HEALING CEMENT-BASED MATERIALS?, in: 2007.

[38] M. Getnet Meharie, Factors Affecting the Self-Healing Efficiency of Cracked Concrete Structures, Am. J. Appl. Sci. Res. 3 (2017) 80. https://doi.org/10.11648/j.ajasr.20170306.12.

[39] D. Snoeck, P.A. Smetryns, N. De Belie, Improved multiple cracking and

autogenous healing in cementitious materials by means of chemically-treated natural fibers, Biosyst. Eng. 139 (2015) 87–99. https://doi.org/10.1016/j.biosystemseng.2015.08.007.

[40] C. Manvith Kumar Reddy, B. Ramesh, D. Macrin, Effect of crystalline admixtures, polymers and fibers on self healing concrete - a review, Mater. Today Proc. 33 (2020) 763–770. https://doi.org/10.1016/j.matpr.2020.06.122.

[41] Y. Qian, Y. Zhou, L. Li, W. Liu, D. Yang, X. Qiu, Facile preparation of active lignin capsules for developing self-healing and UV-blocking polyurea coatings, Prog. Org. Coatings. 138 (2020) 105354. https://doi.org/10.1016/j.porgcoat.2019.105354.

[42] P. Aggarwal, R.P. Singh, Y. Aggarwal, Use of nano-silica in cement based materials—A review, Cogent Eng. 2 (2015). https://doi.org/10.1080/23311916.2015.1078018.

[43] N. Makul, Advanced smart concrete - A review of current progress, benefits and challenges, J. Clean. Prod. 274 (2020) 122899. https://doi.org/10.1016/j.jclepro.2020.122899.

[44] H. Chang, C. Li, J. Wang, H. Zhang, Z. Ge, Z. Zuo, J. Liu, Y. Zhou, The features of different mineral admixtures affecting the self-healing capacity of cementitious-based materials, Constr. Build. Mater. 297 (2021) 123822. https://doi.org/10.1016/j.conbuildmat.2021.123822.

[45] D. Palin, V. Wiktor, H.M. Jonkers, Autogenous healing of marine exposed concrete: Characterization and quantification through visual crack closure, Cem. Concr. Res. 73 (2015) 17–24. https://doi.org/10.1016/j.cemconres.2015.02.021.

[46] L. De Meyst, E. Mannekens, K. Van Tittelboom, N. De Belie, The influence of superabsorbent polymers (SAPs) on autogenous shrinkage in cement paste, mortar and concrete, Constr. Build. Mater. 286 (2021) 122948. https://doi.org/10.1016/j.conbuildmat.2021.122948.

[47] M. Tsuji, K. Shitama, D. Isobe, Basic studies on simplified curing technique, and prevention of initial cracking and leakage of water through cracks of concrete by applying superabsorbent polymers as new concrete admixture, Zair. Soc. Mater. Sci. Japan. 48 (1999) 1308–1315. https://doi.org/10.2472/jsms.48.1308.

[48] C. Schroefl, V. Mechtcherine, P. Vontobel, J. Hovind, E. Lehmann, Sorption kinetics of superabsorbent polymers (SAPs) in fresh Portland cement-based pastes visualized and quantified by neutron radiography and correlated to the

progress of cement hydration, Cem. Concr. Res. 75 (2015) 1–13. https://doi.org/10.1016/j.cemconres.2015.05.001.

[49] P. Minnebo, G. Thierens, G. De Valck, K. Van Tittelboom, N. De Belie, D. Van Hemelrijck, E. Tsangouri, A novel design of autonomously healed concrete: Towards a vascular healing network, Materials (Basel). 10 (2017) 1–23. https://doi.org/10.3390/ma10010049.

[50] W. Li, Z. Jiang, Z. Yang, N. Zhao, W. Yuan, Self-healing efficiency of cementitious materials containing microcapsules filled with healing adhesive: Mechanical restoration and healing process monitored by water absorption, PLoS One. 8 (2013) 1–18. https://doi.org/10.1371/journal.pone.0081616.

[51] S. Guzlena, G. Sakale, Self-healing of glass fiber reinforced concrete (GRC) and polymer glass fiber reinforced concrete (PGRC) using crystalline admixtures, Constr. Build. Mater. 267 (2021) 120963. https://doi.org/10.1016/j.conbuildmat.2020.120963.

[52] J.S. Juan, M.L. Nó, C.A. Schuh, Nanoscale shape-memory alloys for ultrahigh mechanical damping, Nat. Nanotechnol. 4 (2009) 415–419. https://doi.org/10.1038/nnano.2009.142.

[53] W. Chen, B. Lin, K. Feng, S. Cui, D. Zhang, Effect of shape memory alloy fiber content and preloading level on the self-healing properties of smart cementitious composite (SMA-ECC), Constr. Build. Mater. 341 (2022) 127797. https://doi.org/10.1016/j.conbuildmat.2022.127797.

[54] H. Ahmed, Self-healing fungi concrete using potential strains Rhizopus oryzae and Trichoderma longibrachiatum, J. Build. Eng. 50 (2022) 104155. https://doi.org/10.1016/j.jobe.2022.104155.

[55] H.M. Jonkers, E. Schlangen, Crack Repair By Concrete-Immobilized Bacteria, Civ. Eng. (2007) 1–7. http://extras.springer.com/2007/978-1-4020-6250-6/documents/9.pdf.

[56] N. Chahal, R. Siddique, A. Rajor, Influence of bacteria on the compressive strength, water absorption and rapid chloride permeability of fly ash concrete, Constr. Build. Mater. 28 (2012) 351–356. https://doi.org/10.1016/j.conbuildmat.2011.07.042.

[57] B. Madhu Sudana Reddy, D. Revathi, An experimental study on effect of Bacillus sphaericus bacteria in crack filling and strength enhancement of concrete, Mater. Today Proc. 19 (2019) 803–809.

https://doi.org/10.1016/j.matpr.2019.08.135.
[58] V.R. Santhosh K. Ramachandran and Sookie S. Bang, Remediation of Concrete Using Microorganisms, ACI Mater. J. 98 (n.d.). https://doi.org/10.14359/10154.
[59] P. Ghosh, S. Mandal, B.D. Chattopadhyay, S. Pal, Use of microorganism to improve the strength of cement mortar, Cem. Concr. Res. 35 (2005) 1980–1983. https://doi.org/10.1016/j.cemconres.2005.03.005.
[60] H.M. Jonkers, Self Healing Concrete: A Biological Approach, in: S. van der Zwaag (Ed.), Self Heal. Mater. An Altern. Approach to 20 Centuries Mater. Sci., Springer Netherlands, Dordrecht, 2007: pp. 195–204. https://doi.org/10.1007/978-1-4020-6250-6_9.
[61] H.M. Jonkers, Self healing materials, (2007).
[62] H.M. Jonkers, E. Schlangen, A two component bacteria-based self-healing concrete, Concr. Repair, Rehabil. Retrofit. II. (2008) 215–220. https://doi.org/10.1201/9781439828403.ch27.
[63] H. Huang, G. Ye, C. Qian, E. Schlangen, Self-healing in cementitious materials: Materials, methods and service conditions, Mater. Des. 92 (2016) 499–511. https://doi.org/10.1016/j.matdes.2015.12.091.
[64] N. De Belie, J. Wang, Bacteria-based repair and self-healing of concrete, J. Sustain. Cem. Mater. 5 (2016) 35–56. https://doi.org/10.1080/21650373.2015.1077754.
[65] X.F. Wang, Z.H. Yang, C. Fang, N.X. Han, G.M. Zhu, J.N. Tang, F. Xing, Evaluation of the mechanical performance recovery of self-healing cementitious materials – its methods and future development: A review, Constr. Build. Mater. 212 (2019) 400–421. https://doi.org/10.1016/j.conbuildmat.2019.03.117.
[66] S. Bhaskar, K.M. Anwar Hossain, M. Lachemi, G. Wolfaardt, M. Otini Kroukamp, Effect of self-healing on strength and durability of zeolite-immobilized bacterial cementitious mortar composites, Cem. Concr. Compos. 82 (2017) 23–33. https://doi.org/10.1016/j.cemconcomp.2017.05.013.
[67] Y. Al-Salloum, H. Abbas, Q.I. Sheikh, S. Hadi, S. Alsayed, T. Almusallam, Effect of some biotic factors on microbially-induced calcite precipitation in cement mortar, Saudi J. Biol. Sci. 24 (2017) 286–294. https://doi.org/10.1016/j.sjbs.2016.01.016.
[68] L.J.F. Jones, R. Carballido-López, J. Errington, Control of cell shape in bacteria: Helical, actin-like filaments in Bacillus subtilis, Cell. 104 (2001) 913–922.

https://doi.org/10.1016/S0092-8674(01)00287-2.
[69] T.H. Nguyen, E. Ghorbel, H. Fares, A. Cousture, Bacterial self-healing of concrete and durability assessment, Cem. Concr. Compos. 104 (2019) 103340. https://doi.org/10.1016/j.cemconcomp.2019.103340.
[70] W. De Muynck, K. Cox, N. De Belie, W. Verstraete, Bacterial carbonate precipitation as an alternative surface treatment for concrete, Constr. Build. Mater. 22 (2008) 875–885. https://doi.org/10.1016/j.conbuildmat.2006.12.011.
[71] H.M. Jonkers, A. Thijssen, G. Muyzer, O. Copuroglu, E. Schlangen, Application of bacteria as self-healing agent for the development of sustainable concrete, Ecol. Eng. 36 (2010) 230–235. https://doi.org/10.1016/j.ecoleng.2008.12.036.
[72] G.D.O. Okwadha, J. Li, Optimum conditions for microbial carbonate precipitation, Chemosphere. 81 (2010) 1143–1148. https://doi.org/10.1016/j.chemosphere.2010.09.066.
[73] S. Sujatha, K. Sarayu, M. Annaselvi, R.M. A, R.K. V, N.R. Iyer, Soil Bacteria for the Strength Enhancement of Cement Mortar, 4 (2014) 51–54. https://doi.org/10.5923/c.jce.201401.10.
[74] S. Ghosh, G. Korza, M. Maciejewski, P. Setlow, Analysis of metabolism in dormant spores of Bacillus species by 31P nuclear magnetic resonance analysis of low-molecular-weight compounds, J. Bacteriol. 197 (2015) 992–1001. https://doi.org/10.1128/JB.02520-14.
[75] J. Xu, W. Yao, Multiscale mechanical quantification of self-healing concrete incorporating non-ureolytic bacteria-based healing agent, Cem. Concr. Res. 64 (2014) 1–10. https://doi.org/10.1016/j.cemconres.2014.06.003.
[76] S. Achuthan, Bacterial Self Healing Concrete-an Innovative Repair Technique, (2019). www.ripublication.comijaer.htm.
[77] M. Luo, C.X. Qian, R.Y. Li, Factors affecting crack repairing capacity of bacteria-based self-healing concrete, Constr. Build. Mater. 87 (2015) 1–7. https://doi.org/10.1016/j.conbuildmat.2015.03.117.
[78] M. Luo, C. Qian, Influences of bacteria-based self-healing agents on cementitious materials hydration kinetics and compressive strength, Constr. Build. Mater. 121 (2016) 659–663. https://doi.org/10.1016/j.conbuildmat.2016.06.075.
[79] C. Lors, J. Ducasse-Lapeyrusse, R. Gagné, D. Damidot, Microbiologically induced calcium carbonate precipitation to repair microcracks remaining after

autogenous healing of mortars, Constr. Build. Mater. 141 (2017) 461–469. https://doi.org/10.1016/j.conbuildmat.2017.03.026.

[80] K.K. Sahoo, A.K. Sathyan, C. Kumari, P. Sarkar, R. Davis, Investigation of cement mortar incorporating Bacillus sphaericus, Int. J. Smart Nano Mater. 7 (2016) 91–105. https://doi.org/10.1080/19475411.2016.1205157.

[81] S. Joshi, S. Goyal, A. Mukherjee, M.S. Reddy, Protection of concrete structures under sulfate environments by using calcifying bacteria, Constr. Build. Mater. 209 (2019) 156–166. https://doi.org/10.1016/j.conbuildmat.2019.03.079.

[82] Á.T. Kovács, Bacillus subtilis., Trends Microbiol. 27 (2019) 724–725. https://doi.org/10.1016/j.tim.2019.03.008.

[83] N. Schwantes-Cezario, L.P. Medeiros, A.G. De Oliveira, G. Nakazato, R. Katsuko Takayama Kobayashi, B.M. Toralles, Bioprecipitation of calcium carbonate induced by Bacillus subtilis isolated in Brazil, Int. Biodeterior. Biodegrad. 123 (2017) 200–205. https://doi.org/10.1016/j.ibiod.2017.06.021.

[84] S. Mondal, A. (Dey) Ghosh, Spore-forming Bacillus subtilis vis-à-vis non-spore-forming Deinococcus radiodurans, a novel bacterium for self-healing of concrete structures: A comparative study, Constr. Build. Mater. 266 (2021) 121122. https://doi.org/10.1016/j.conbuildmat.2020.121122.

[85] J. Wang, K. Van Tittelboom, N. De Belie, W. Verstraete, Use of silica gel or polyurethane immobilized bacteria for self-healing concrete, Constr. Build. Mater. 26 (2012) 532–540. https://doi.org/10.1016/j.conbuildmat.2011.06.054.

[86] H. Chen, C. Qian, H. Huang, Self-healing cementitious materials based on bacteria and nutrients immobilized respectively, Constr. Build. Mater. 126 (2016) 297–303. https://doi.org/10.1016/j.conbuildmat.2016.09.023.

[87] A.N. Ede, O.M. Olofinnade, O. Joshua, D.O. Nduka, O.A. Oshogbunu, Influence of bamboo fiber and limestone powder on the properties of self-compacting concrete, Cogent Eng. 7 (2020). https://doi.org/10.1080/23311916.2020.1721410.

[88] J. Xu, X. Wang, Self-healing of concrete cracks by use of bacteria-containing low alkali cementitious material, Constr. Build. Mater. 167 (2018) 1–14. https://doi.org/10.1016/j.conbuildmat.2018.02.020.

[89] H. Xu, J. Lian, M. Gao, D. Fu, Y. Yan, Self-Healing Concrete Using Rubber Particles to Immobilize Bacterial Spores, Materials (Basel). 12 (2019) 2313. https://doi.org/10.3390/ma12142313.

[90] K. Vijay, M. Murmu, Self-repairing of concrete cracks by using bacteria and basalt fiber, SN Appl. Sci. 1 (2019) 1–10. https://doi.org/10.1007/s42452-019-1404-5.

[91] J. Feng, Y. Su, C. Qian, Coupled effect of PP fiber, PVA fiber and bacteria on self-healing efficiency of early-age cracks in concrete, Constr. Build. Mater. 228 (2019) 116810. https://doi.org/10.1016/j.conbuildmat.2019.116810.

[92] Y. Su, C. Qian, Y. Rui, J. Feng, Exploring the coupled mechanism of fibers and bacteria on self-healing concrete from bacterial extracellular polymeric substances (EPS), Cem. Concr. Compos. 116 (2021). https://doi.org/10.1016/j.cemconcomp.2020.103896.

[93] Y. Su, C. Qian, Y. Rui, J. Feng, Exploring the coupled mechanism of fibers and bacteria on self-healing concrete from bacterial extracellular polymeric substances (EPS), Cem. Concr. Compos. 116 (2021) 103896. https://doi.org/10.1016/j.cemconcomp.2020.103896.

[94] S.R. Ferreira, L.E. Silva, Z. McCaffrey, C. Ballschmiede, E. Koenders, Effect of elevated temperature on sisal fibers degradation and its interface to cement based systems, Constr. Build. Mater. 272 (2021) 121613. https://doi.org/10.1016/j.conbuildmat.2020.121613.

[95] N.K. Krishna, M. Prasanth, R. Gowtham, S. Karthic, K.M. Mini, Enhancement of properties of concrete using natural fibers, Mater. Today Proc. 5 (2018) 23816–23823. https://doi.org/10.1016/j.matpr.2018.10.173.

[96] J.E. Fernandez, Flax fiber reinforced concrete - A natural fiber biocomposite for sustainable building materials, High Perform. Struct. Mater. 4 (2002) 193–207.

[97] P.P. Yalley, A.S.. Kwan, Coconut Fiber as Enhancement of Concrete, J. Eng. Technol. 2 (2012) 54–73.

[98] A. Razmi, M.M. Mirsayar, On the mixed mode I/II fracture properties of jute fiber-reinforced concrete, Constr. Build. Mater. 148 (2017) 512–520. https://doi.org/10.1016/j.conbuildmat.2017.05.034.

[99] O. Onuaguluchi, N. Banthia, Plant-based natural fiber reinforced cement composites: A review, Cem. Concr. Compos. 68 (2016) 96–108. https://doi.org/10.1016/j.cemconcomp.2016.02.014.

[100] S.R. Ferreira, M. Pepe, E. Martinelli, F. de Andrade Silva, R.D. Toledo Filho, Influence of natural fibers characteristics on the interface mechanics with cement based matrices, Compos. Part B Eng. 140 (2018) 183–196.

https://doi.org/10.1016/j.compositesb.2017.12.016.
[101] L. Mbereyaho, F. Twayigize, L.G.M. Ishimwe, S. Mutumwinka, Experimental investigation on the potentials of Sisal Fibers as Reinforcements for Drainage Concrete Cover Plates, Rwanda J. Eng. Sci. Technol. Environ. 3 (2020) 1–12. https://doi.org/10.4314/rjeste.v3i1.9.
[102] S. Solai Mathi, S. Karthikeyan, V. Johnpaul, P.R. Riyas, N. Chidambaram, M. Vegumathi, Experimental investigation on self compacting concrete with sisal fiber, Mater. Today Proc. (2021). https://doi.org/10.1016/j.matpr.2020.10.1011.
[103] Tunje Constance, R. Onchiri, J. Thuo, Concrete Microstructure Study on the Effect of Sisal Fiber Addition on Sugarcane Bagasse Ash Concrete, Open Civ. Eng. J. 15 (2021) 320–329. https://doi.org/10.2174/1874149502115010320.
[104] T.D.P. Thao, T.J.S. Johnson, Q.S. Tong, P.S. Dai, Implementation of self-healing in concrete–Proof of concept, IES J. Part A Civ. Struct. Eng. 2 (2009) 116–125. https://doi.org/10.1080/19373260902843506.
[105] K. Van Tittelboom, N. De Belie, D. Van Loo, P. Jacobs, Self-healing efficiency of cementitious materials containing tubular capsules filled with healing agent, Cem. Concr. Compos. 33 (2011) 497–505. https://doi.org/10.1016/j.cemconcomp.2011.01.004.
[106] E. Cuenca, A. Tejedor, L. Ferrara, A methodology to assess crack-sealing effectiveness of crystalline admixtures under repeated cracking-healing cycles, Constr. Build. Mater. 179 (2018) 619–632. https://doi.org/10.1016/j.conbuildmat.2018.05.261.
[107] ASTM C150, ASTM C150/C150M - 18 Standard Specifications for Portland Cement, i (1999) 1–9. https://doi.org/10.1520/C0150.
[108] ASTM C33, Concrete Aggregates 1, i (2010) 1–11. https://doi.org/10.1520/C0033.
[109] ASTM, Método de prueba estándar para Densidad Relativa (Gravedad Específica) y Absorción de Agregado Grueso, ASTM C127-15, (2015) 1–5. https://doi.org/10.1520/C0127-15.2.
[110] ASTM C-128-15, Standard Test Method for Relative Density (Specific Gravity) and Absorption of Fine Aggregates, ASTM International, West Conshohocken, PA, 2015, ASTM Int. i (2015) 15–20. https://doi.org/10.1520/C0128-15.2.
[111] A.R. Martin, M.A. Martins, O.R.R.F. Da Silva, L.H.C. Mattoso, Studies on the thermal properties of sisal fiber and its constituents, Thermochim. Acta. 506

(2010) 14–19. https://doi.org/10.1016/j.tca.2010.04.008.

[112] R.R.M. de Freitas, K.P. do Carmo, J. de Souza Rodrigues, V.H. de Lima, J. Osmari da Silva, V.R. Botaro, Influence of alkaline treatment on sisal fiber applied as reinforcement agent in composites of corn starch and cellulose acetate matrices, Plast. Rubber Compos. 50 (2021) 9–17. https://doi.org/10.1080/14658011.2020.1816119.

[113] S. Z, R. El, Identification of the Physical and Mechanical Properties of Composite Materials, (2021).

[114] P.R.L. Lima, H.M. Santos, G.P. Camilloto, R.S. Cruz, Effect of surface biopolymeric treatment on sisal fiber properties and fiber-cement bond, J. Eng. Fiber. Fabr. 12 (2017) 59–71. https://doi.org/10.1177/155892501701200207.

[115] A. Orue, A. Jauregi, C. Peña-Rodriguez, J. Labidi, A. Eceiza, A. Arbelaiz, The effect of surface modifications on sisal fiber properties and sisal/poly (lactic acid) interface adhesion, Compos. Part B Eng. 73 (2015) 132–138. https://doi.org/10.1016/j.compositesb.2014.12.022.

[116] J. Samuel, M.L. Paul, H. Ravishankar, A. Mathur, D.P. Saha, C. Natarajan, A. Mukherjee, The differential stress response of adapted chromite mine isolates Bacillus subtilis and Escherichia coli and its impact on bioremediation potential, Biodegradation. 24 (2013) 829–842. https://doi.org/10.1007/s10532-013-9631-8.

[117] Z. Filip, S. Herrmann, J. Kubat, FT-IR spectroscopic characteristics of differently cultivated Bacillus subtilis, Microbiol. Res. 159 (2004) 257–262. https://doi.org/10.1016/j.micres.2004.05.002.

[118] N. Haddad, J. Wang, B. Mu, Identification of a Biosurfactant Producing Strain: Bacillus subtilis HOB2, Protein Pept. Lett. 16 (2009) 7–13. https://doi.org/10.2174/092986609787049358.

[119] R. Harish, J. Samuel, R. Mishra, N. Chandrasekaran, A. Mukherjee, Bio-reduction of Cr(VI) by exopolysaccharides (EPS) from indigenous bacterial species of Sukinda chromite mine, India, Biodegradation. 23 (2012) 487–496. https://doi.org/10.1007/s10532-011-9527-4.

[120] ASTM C-39, Standard Test Method for Compressive Strength of Cylindrical Concrete Specimens 1 This standard is for EDUCATIONAL USE ONLY ., Annu. B. ASTM Stand. (2010) 1–7. https://doi.org/10.1520/C0039.

[121] ASTM C469-11, Standard Test Method for Splitting Tensile Strength of

Cylindrical Concrete Specimens, Man. Hydrocarb. Anal. 6th Ed. i (2008) 545-545–3. https://doi.org/10.1520/C0496.

[122] A. Standard, C1585-13, Stand. Test Method Meas. Rate Absorpt. Water by Hydraul. Concr. ASTM Int. 41 (2013) 1–6. https://doi.org/10.1520/C1585-13.2.

[123] B. Dong, G. Fang, W. Ding, Y. Liu, J. Zhang, N. Han, F. Xing, Self-healing features in cementitious material with urea-formaldehyde/epoxy microcapsules, Constr. Build. Mater. 106 (2016) 608–617. https://doi.org/10.1016/j.conbuildmat.2015.12.140.

[124] J. Liu, C. Lv, Research Progress on Durability of Cellulose Fiber-Reinforced Cement-Based Composites, Int. J. Polym. Sci. 2021 (2021). https://doi.org/10.1155/2021/1014531.

[125] J. Flores-rada, Reinforced Concrete Properties, (2022) 1–18.

[126] G. Ren, B. Yao, H. Huang, X. Gao, Influence of sisal fibers on the mechanical performance of ultra-high performance concretes, Constr. Build. Mater. 286 (2021) 122958. https://doi.org/10.1016/j.conbuildmat.2021.122958.

[127] C.C. Agbim, Concrete reinforced with glass fibers, Mag. Concr. Res. 16 (1964) 195–202. https://doi.org/10.1680/macr.1964.16.49.195.

[128] S. Jena, B. Basa, K.C. Panda, N.K. Sahoo, Impact of Bacillus subtilis bacterium on the properties of concrete, Mater. Today Proc. 32 (2020) 651–656. https://doi.org/10.1016/j.matpr.2020.03.129.

[129] N. Nain, R. Surabhi, N. V. Yathish, V. Krishnamurthy, T. Deepa, S. Tharannum, Enhancement in strength parameters of concrete by application of Bacillus bacteria, Constr. Build. Mater. 202 (2019) 904–908. https://doi.org/10.1016/j.conbuildmat.2019.01.059.

[130] B. Ali, H. Ahmed, L.A. Qureshi, R. Kurda, H. Hafez, H. Mohammed, A. Raza, Enhancing the hardened properties of recycled concrete (RC) through synergistic incorporation of fiber reinforcement and silica fume, Materials (Basel). 13 (2020) 1–19. https://doi.org/10.3390/ma13184112.

[131] M. Pommet, J. Juntaro, J.Y.Y. Heng, A. Mantalaris, A.F. Lee, K. Wilson, G. Kalinka, M.S.P. Shaffer, A. Bismarck, Surface modification of natural fibers using bacteria: Depositing bacterial cellulose onto natural fibers to create hierarchical fiber reinforced nanocomposites, Biomacromolecules. 9 (2008) 1643–1651. https://doi.org/10.1021/bm800169g.

[132] J.Y. Wang, H. Soens, W. Verstraete, N. De Belie, Self-healing concrete by use

of microencapsulated bacterial spores, Cem. Concr. Res. 56 (2014) 139–152. https://doi.org/10.1016/j.cemconres.2013.11.009.

[133] R.A. Khushnood, A. Arif, N. Shaheen, A.G. Zafar, T. Hassan, M. Akif, Bio-inspired self-healing and self-sensing cementitious mortar using Bacillus subtilis immobilized on graphitic platelets, Constr. Build. Mater. 316 (2022) 125818. https://doi.org/10.1016/j.conbuildmat.2021.125818.

[134] R.A. Khushnood, S. ud din, N. Shaheen, S. Ahmad, F. Zarrar, Bio-inspired self-healing cementitious mortar using Bacillus subtilis immobilized on nano-/micro-additives, J. Intell. Mater. Syst. Struct. 30 (2019) 3–15. https://doi.org/10.1177/1045389X18806401.

[135] N. Shaheen, R.A. Khushnood, S. Ud Din, Bioimmobilized Limestone Powder for Autonomous Healing of Cementitious Systems: A Feasibility Study, Adv. Mater. Sci. Eng. 2018 (2018). https://doi.org/10.1155/2018/7049121.

[136] L. Xu, B. Li, X. Ding, Y. Chi, C. Li, B. Huang, Y. Shi, Experimental Investigation on Damage Behavior of Polypropylene Fiber Reinforced Concrete under Compression, Int. J. Concr. Struct. Mater. 12 (2018). https://doi.org/10.1186/s40069-018-0302-3.

[137] O. Gouda, A. Hassanein, T. Youssef, K. Galal, Stress-Strain Behaviour of Masonry Prisms Constructed with Glass Fiber-Reinforced Grout, Constr. Build. Mater. 267 (2021) 120984. https://doi.org/10.1016/j.conbuildmat.2020.120984.

[138] Y. Wang, S. Gao, W. Li, Study on Compression Deformation and Damage Characteristics of Pine Needle Fiber-Reinforced Concrete Using DIC, Materials (Basel). 15 (2022). https://doi.org/10.3390/ma15051654.

[139] S. Gupta, Comparison of improved autogenous and bio-based self-healing techniques in fiber-reinforced mortar: Effect of bacteria incorporation strategy and fiber hybridization, J. Build. Eng. 45 (2022) 103607. https://doi.org/10.1016/j.jobe.2021.103607.

[140] W. Zhong, W. Yao, Influence of damage degree on self-healing of concrete, Constr. Build. Mater. 22 (2008) 1137–1142. https://doi.org/10.1016/j.conbuildmat.2007.02.006.

[141] M.N. Amin, A. Ahmad, K. Shahzada, K. Khan, F.E. Jalal, M.G. Qadir, Mechanical and microstructural performance of concrete containing high-volume of bagasse ash and silica fume, Sci. Rep. 12 (2022) 1–21. https://doi.org/10.1038/s41598-022-08749-1.

[142] D. Pan, S.A. Yaseen, K. Chen, D. Niu, C.K. Ying Leung, Z. Li, Study of the influence of seawater and sea sand on the mechanical and microstructural properties of concrete, J. Build. Eng. 42 (2021) 103006. https://doi.org/10.1016/j.jobe.2021.103006.

[143] V. Singh Kashyap, U. Agrawal, K. Arora, G. Sancheti, FTIR Analysis of Nanomodified Cement Concrete Incorporating Nano Silica and Waste Marble Dust, IOP Conf. Ser. Earth Environ. Sci. 796 (2021). https://doi.org/10.1088/1755-1315/796/1/012022.

[144] I. García Lodeiro, D.E. Macphee, A. Palomo, A. Fernández-Jiménez, Effect of alkalis on fresh C-S-H gels. FTIR analysis, Cem. Concr. Res. 39 (2009) 147–153. https://doi.org/10.1016/j.cemconres.2009.01.003.

[145] Q. Zhan, X. Yu, Z. Pan, C. Qian, Microbial-induced synthesis of calcite based on carbon dioxide capture and its cementing mechanism, J. Clean. Prod. 278 (2021) 123398. https://doi.org/10.1016/j.jclepro.2020.123398.

[146] Y. Yue, Y. Bai, J.J. Wang, Application of raman spectroscopy for tracing the status of silica fume in cementitious materials, Int. Conf. Durab. Concr. Struct. ICDCS 2016. (2016) 174–178. https://doi.org/10.5703/1288284316128.

[147] M. Vetter, J. Gonzalez-Rodriguez, E. Nauha, T. Kerr, The use of Raman spectroscopy to monitor phase changes in concrete following high temperature exposure, Constr. Build. Mater. 204 (2019) 450–457. https://doi.org/10.1016/j.conbuildmat.2019.01.165.

[148] J. Skibsted, C. Hall, Characterization of cement minerals, cements and their reaction products at the atomic and nano scale, Cem. Concr. Res. 38 (2008) 205–225. https://doi.org/10.1016/j.cemconres.2007.09.010.

[149] T. Mi, Y. Li, W. Liu, W. Li, W. Long, Z. Dong, Q. Gong, F. Xing, Y. Wang, Quantitative evaluation of cement paste carbonation using Raman spectroscopy, Npj Mater. Degrad. 5 (2021). https://doi.org/10.1038/s41529-021-00181-6.

[150] M. De La Pierre, C. Carteret, L. Maschio, E. André, R. Orlando, R. Dovesi, The Raman spectrum of CaCO3 polymorphs calcite and aragonite: A combined experimental and computational study, J. Chem. Phys. 140 (2014). https://doi.org/10.1063/1.4871900.

[151] O.S. Vereshchagin, O. V. Frank-Kamenetskaya, K. V. Shumilova, N.Y. Khadeeva, Carbonate sediments on decorative fountains in Peterhof, Russia, Environ. Earth Sci. 77 (2018) 1–10. https://doi.org/10.1007/s12665-018-7243-7.

[152] F.C. Donnelly, F. Purcell-Milton, V. Framont, O. Cleary, P.W. Dunne, Y.K. Gun'ko, Synthesis of CaCO3 nano- and micro-particles by dry ice carbonation, Chem. Commun. 53 (2017) 6657–6660. https://doi.org/10.1039/c7cc01420a.

[153] D. Homma, H. Mihashi, T. Nishiwaki, Self-healing capability of fiber reinforced cementitious composites, J. Adv. Concr. Technol. 7 (2009) 217–228. https://doi.org/10.3151/jact.7.217.